Renewable and Sustainable Energy Reviews 101 (2019) 82–102

Contents lists available at ScienceDirect

Renewable and Sustainable Energy Reviews

journal homepage: www.elsevier.com/locate/rser

Power tracking techniques for efficient operation of photovoltaic array in solar applications – A review

Riaz Ahmad[a,*], Ali F. Murtaza[a], Hadeed Ahmed Sher[b]

[a] Faculty of Engineering, Electrical Engineering Department, University of Central Punjab, Lahore, Pakistan
[b] Faculty of Electrical Engineering, Ghulam Ishaq Khan Institute of Engineering Sciences and Technology, Topi, Pakistan

ARTICLE INFO

Keywords:
Photovoltaic system
MPPT techniques
Conventional methods
Partial shading
Bio-inspired algorithms

ABSTRACT

This paper presents a comprehensive overview on various maximum power point tracking (MPPT) techniques, which have been recently designed, simulated and/or experimentally validated in the PV literature. The primary goal of each MPPT technique is to optimize the output of shaded/unshaded photovoltaic (PV) array under static and dynamic weather conditions. Though each MPPT technique has its own pros and cons, an optimized MPPT technique is characterized in many aspects like hardware and software simplicity, implementation, cost effectiveness, sensors required, popularity, accuracy and convergence speed. In this paper the rating of various MPPT methods has been done based on the benchmark P&O method. The rating criteria is separately calculated for the techniques that are capable to work in full-sun and partial shading conditions. A rule based table is set to evaluate the MPPT against the algorithm's complexity, hardware implementation, tracking speed, and steady state accuracy or detection of global maximum. Moreover, special consideration has been given to bio-inspired MPPT algorithms. The bio-inspired algorithms are compared side by side with their specific application in PV system. A tree diagram is also designed to see the emergence of partial shading algorithms over a period of time. The traits presented in this paper are novel and provide bottom-line for the researchers to select and implement an appropriate MPPT technique.

1. Introduction

The worldwide energy demand is increasing on a faster pace than the energy generation because of enhanced industrialization, growing population and improved living standards. According to international energy agency (IEA) reports, the energy consumption of world will increase by 44% from 2006 to 2030 [1]. In the present scenario, the fossil fuels such as oil, gas and coal are depleting with every passing day, which are the primary energy drivers and pollution contributors [2–4]. Therefore, the world is moving to new energy resources, which are promising, socially compatible, renewable, and sustainable. These sources are solar, wind, biomass, small hydro, geothermal, and ocean tidal/thermal.

Photovoltaic (PV) is a prominent renewable energy source due to its sustainability, local availability, environmental friendly nature, simple technology, increasing cost effectiveness and less balance of systems. In photovoltaic, the sunlight is converted into direct current using semiconductor materials without any moving parts and carbon emissions. For the past decades, the power generation from PV systems have showed extensive penetration in commercial and domestic facilities. PV has now turned into the third most essential renewable energy source after hydro and wind. At present, more than 100 nations are utilizing ground mounted or building integrated PV systems for domestic, commercial and grid applications. According to IEA-PVPS (international energy agency for photovoltaic power systems), the worldwide installed PV capacity has expanded to 227 GW in March 2015 and is expected to reach up to 500 GW by the end of 2020 [5,6].

The current-voltage (I-V) curve of PV array relies on irradiance and temperature conditions. When the irradiance increases with constant temperature, the photovoltaic current also increases in direct proportion with negligible effect on PV voltage. Similarly, if the temperature increases with constant irradiance, the PV voltage decreases substantially while the PV current increases slightly. Under uniform condition, PV array exhibits unique maximum power point (MPP) on its I-V curve. The tracking mechanism in PV system, known as maximum power point tracking (MPPT) technique, is inevitable to search the MPP as innate characteristic of PV varies non-linearly with irradiance, temperature, and load. The matter becomes further complicated when PV array is under the influence of partial shading. During this condition, modules receive contrasted irradiance levels and multiple local

* Corresponding author.
E-mail address: rana.riaz@ucp.edu.pk (R. Ahmad).

https://doi.org/10.1016/j.rser.2018.10.015
Received 6 November 2017; Received in revised form 8 October 2018; Accepted 13 October 2018
1364-0321/ © 2018 Elsevier Ltd. All rights reserved.

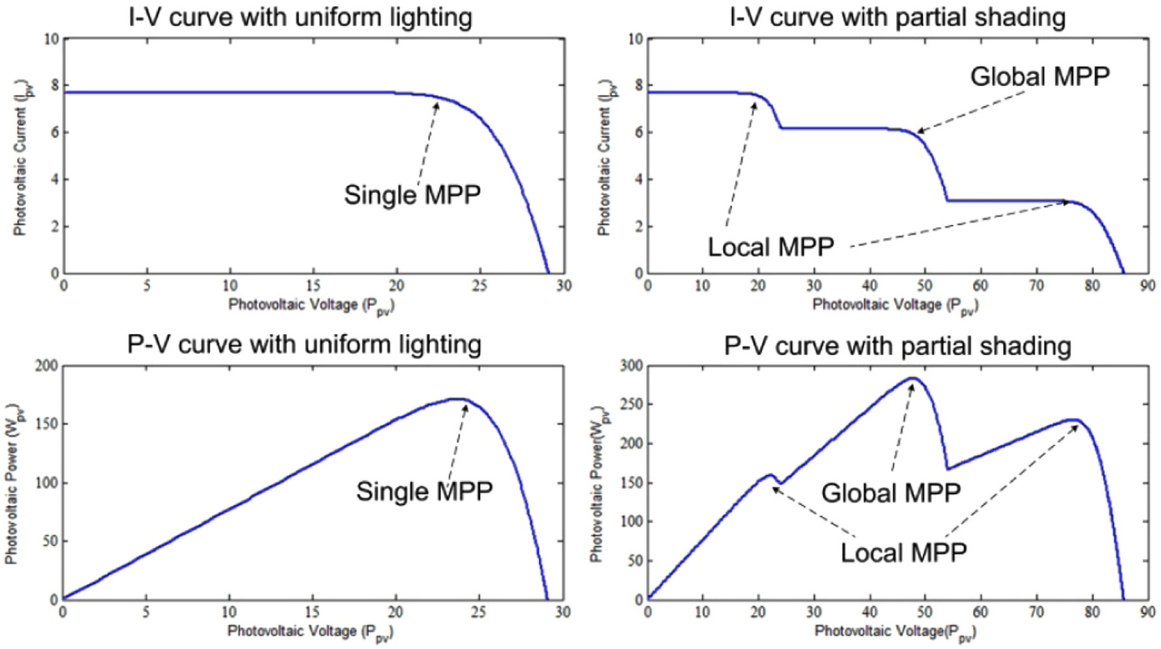

Fig. 1. Characteristic curves of a typical PV module under full-sun(uniform lighting) and partial shading condition.

maxima (LMs) start appearing on I-V curve due to action of bypass diodes as shown in Fig. 1. A bypass diode is always connected across the groups of 16–18 cells to avoid the adverse effects of hot-spots phenomenon. Consequently, a more hi-tech and sophisticated MPPT is required for partial shading as compared to uniform condition. MPPTs take the support of power electronic converter to maintain the optimal operating condition of PV array. The converter is installed between the array and load. Whenever MPPT wants to vary the operating point of PV array, it is executed through the capability of converter which alters the output impedance seen by the array. And, at MPP, the output impedance matches the internal impedance of PV array. Generally arguing, an ideal MPPT technique will have the following properties:

1) It has the capability to distinguish between uniform and partial shading conditions
2) It can track MPP instantaneously under uniform weather condition
3) It can search the global maximum under all kinds of partial shading patterns
4) It has a robust tracking speed

For both uniform and partial shading conditions, MPPT designers adopt distinct strategies, which can be characterized as: reconfigurable PV array based MPPTs [7–10], module integrated MPPTs [11–13], MPPTs based on PV array behavior [14–16], MPPTs incited from artificial intelligence concepts or bio-inspired algorithms [17,18]. From these categories, the last two categories are under the scope of this paper as they are considered as superior in terms least hardware requirement [19]. Generally speaking, researchers develop novel ways to track MPP to solve the following basic issues.

1) Enhancing the tracking speed
2) Avoiding confusion in partial shading issues
3) Making the system cost effective
4) Ironing out the basic deficiencies of conventional algorithms

Keeping in view the extensive on-going research of MPPT development, there are several constraints such as algorithm's complexity, hardware implementation, tracking speed, and steady state accuracy or global maximum detection, which can lead PV researchers and designers to confusion in selecting MPPT technique for a specific application. Thus, a comprehensive and an analytical study on the working principles plus pros and cons of all these MPPT techniques is needed. Besides that, a proper ranking criteria with numeric merits and demerits is required to find out the true effective value of the MPPT.

2. MPPT selection criteria

Whenever a new MPPT is published, the effectiveness of the method is established based on following four factors:

- Algorithm's complexity – For both uniform and partial shading conditions
- Hardware implementation – For both uniform and partial shading conditions
- Tracking speed (convergence time) – For both uniform and partial shading conditions
- Steady-state efficiency for uniform condition and accuracy of global maximum detection for partial shading.

The first two factors determine the implementation cost of the MPPT.

2.1. Algorithm's complexity (AC)

The basic benchmark of algorithm's complexity is set at the level of P&O, the flowchart of which is shown in Fig. 2. Worth mentioning here

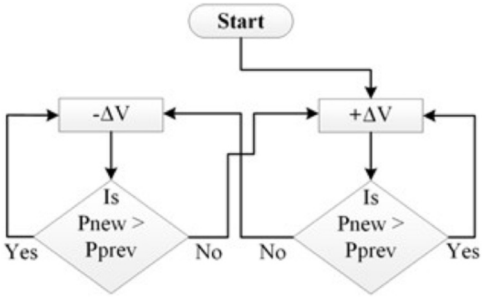

Fig. 2. Flowchart of basic P&O algorithm.

Table 1
Criterion to determine the ranking of MPPTs.

Traits	Grades	Ranking
Algorithm's complexity (AC)	1: Equivalent to P&O	Best
	+1: Minor modifications in P&O	
	+2: Hybrid MPPT i.e. combination of P&O and others or complex relations involved	
	+3: Basic level of artificial intelligence (AI) or bio-inspired (Bio-I) or algorithm containing formulas/relations of similar complexity	
	+4: Modified or advanced level of AI or Bio-I	Worst
Hardware implementation (HI)	1: Conventional dc-dc converter with *I* and *V* sensor	Best
	+1: Modification in dc-dc converter or extra circuit is required with additional *I* or *V* sensor	
	+2: PI/PID controller is used for duty cycle modulation of converter	
	+3: A high-tech embedded system (high-crystal speed), large memory, and analog to digital (A-D) converter with fast sampling rate	
	+4: Irradiance sensor and temperature measurements are used	Worst
Tracking Speed (TS)	1: From 0 ms to 100 ms (Converter's rate: **50 ms, ms:millisec**onds)	Best
	2: From 100 ms to few hundreds of ms	
	3: From few hundreds of ms to seconds	Worst
Steady-state efficiency (SS-E) for uniform condition only	1: From 97% to ≈100%	Best
	2: From 93% to 96.9%	
	3: Less than 92.9%	Worst
Accuracy of global maximum (A-GM) detection for partial shading condition only	1: Detects global maximum with distinct irradiance and temperature conditions - Performance better than MPPT of similar complexity	Best
	2: Tendency of getting caught in local maximum with some shading conditions - Performance better than P&O	
	3: Regularly caught in the local maximum like P&O	Worst

that majority of MPPTs utilize the perturb and observe mechanism in one form or the other. For instance, even the simplest MPPT based on voltage controller will perturb the voltage and observe the error. That's why P&O is considered as baseline, since all the relative grading schemes require some baseline value. The quantitative assessment of MPPTs based on a scale of 1 – 5 is illustrated in Table 1, where grade 1 means the best. If algorithm's complexity of MPPT is near to perturb and observe (P&O), it is graded as 1. Any algorithm enters into artificial intelligence or bio-inspired algorithm domain will get a grade of 4 i.e., + 3 in P&O or more.

2.2. Hardware implementation (HI)

Likewise algorithm's complexity, Fig. 3 shows the schematic diagram for the implementation of basic P&O. It requires a conventional dc-dc converter with only current (*I*) and voltage (*V*) sensors. If an MPPT utilizes the similar setup, it is awarded with a grade of 1. An addition of + 1 (grade 2) means modifications in dc-dc converter or extra circuit is required with an additional *I/V* sensor. If MPPT utilizes the conventional controller (PI/PID etc) for duty-cycle control, + 2 will be added. If MPPT demands sophisticated embedded system with high memory system and crystal frequency, + 3 will be added in the grade. Any involvement of irradiance sensor (pyrometer) plus temperature measurements will lead to the maximum complexity. Note that if MPPT modifies the dc-dc converter and it uses the PI controller, then the grade of MPPT becomes: 1(basic) + 1 (modification in converter) + 2 (Use of PI controller) = 4.

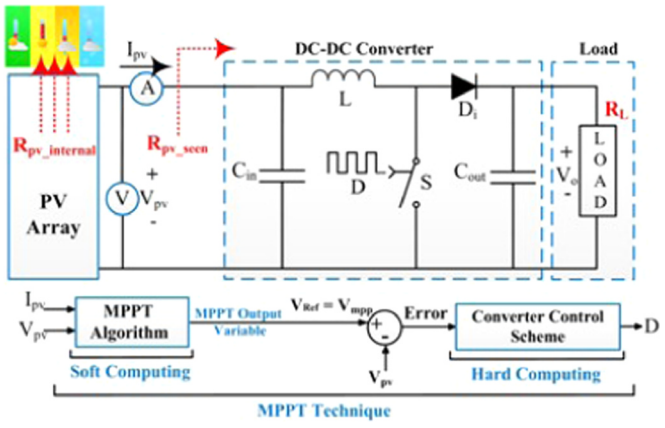

Fig. 3. Basic schematic layout of P&O algorithm implementation.

2.3. Tracking speed

The tracking speed of an algorithm is measured in milliseconds (ms) as it is considered as a common measuring unit amongst the MPPTs. A scale of 1–3 is planted for tracking speed, where if an algorithm achieves the MPP/GM in less than 100 ms, a grade 1 is awarded. The remaining grade information can be deduced from Table 1.

2.4. Steady-state efficiency for uniform condition (SS-E)

Under steady state condition, the efficiency of an MPPT depends upon the ideal power that can be obtained versus the actual power harnessed. If the steady state efficiency is greater than 97% then it is considered the best i.e. 1, between 90% and 97% the tracking efficiency is rated as good, and below 90% the technique is rated as worst i.e. 3.

2.5. Accuracy of global maximum (GM) detection for partial shading (A-GM)

Under the partial shading conditions, if MPPT algorithm is regularly caught in the local maximum (LM) and shows behavior similar to P&O, it is awarded with grade 3. In case, the algorithm gets caught in LM with some shading patterns, the in-between grade is allocated i.e. 2. The rating of MPPT is the best (grade 1), if it successfully identifies the GM regardless of shading pattern and weather conditions. The details are mentioned in Table 1.

2.6. Rating computation of MPPT

The final rating of the MPPT is calculated from the weighted mean formula, where, Eq. (1) and Eq. (2) represent the formula for uniform and partial shading conditions respectively. Since MPPTs are always designed with emphasis on convergence speed and MPP/GM detection, double weightage is given to both traits. Also, this will normalize the relations as TS and SS-E/A-GM vary from 0 to 3, while others vary from 0 to 5.

$$Rating_{MPPT\_Uniform} = \frac{(1\times AC) + (1\times HI) + (2\times TS) + (2\times SS - E)}{6} \quad (1)$$

$$Rating_{MPPT\_Partial} = \frac{(1\times AC) + (1\times HI) + (2\times TS) + (2\times A - GM)}{6} \quad (2)$$

3. MPPT techniques

The MPPT methods studied in this paper are broadly classified into two categories: full-sun and partial shading methods. These two methods are further classified into various categories based on the principle of operation. It is pertinent to mention that sometimes the full-sun methods and the partial shading method are often combined to form a hybrid MPPT method. The purpose of hybrid MPPT method is to enhance the MPPT performance of the conventional MPPT method. However, keeping in view the general practice of researchers and trend of past MPPT surveys, the MPPTs are segmented into two categories.

3.1. Full-sun/uniform condition MPPT

These methods are capable of tracking the MPP only when the irradiance on the PV array is uniform. These methods are simple in design and easy to implement. The further sub-categories of this domain are as follows:

3.1.1. Fractional MPPT methods

Two methods are reported in this domain

- Fractional short circuit current based MPPT (FSCC)
- Fractional open circuit voltage based MPPT (FOCV)

Fig. 4 shows the general block diagram to implement these methods. The input parameter is referred as an off-line parameter, which is either the measured value of short circuit current (I_{sc}) or the open circuit voltage (V_{oc}). The off-line parameter is continuously compared with the photovoltaic current I_{pv} or voltage V_{pv}. The difference is sent to PI controller that tunes the duty cycle of the converter accordingly. These methods require only one sensor to work, hence they are cheap and can be implemented either by using analog or digital circuitry.

3.1.1.1. Fractional short circuit current (FSCC) based MPPT. In literature, it is also termed as short current pulse MPPT [20] or the fractional short circuit current (FSCC) MPPT. It is observed in the I-V curve of the PV module that the current at MPP (I_{mpp}) occurs at the vicinity of short circuit current I_{sc} under any given environmental condition. The relationship between these currents is shown in Eq. (3) [21].

$$I_{mpp} = k_i I_{sc} \quad (3)$$

where, k_i is a constant and typically varies between 0.75 and 0.9. The control flow of setting of PV array at I_{mpp} is depicted in Fig. 4. This method is well suited for high voltage low current applications [22]. Eq. (3) reveals that this method is only an approximation, and therefore it does not operate at exact MPP. Moreover, the full day operation requires intermittent measurements of I_{sc}, which accounts for a power loss. Nevertheless, it has a good efficiency of up to 90% as reported in [23]. In [24], an intelligent FSCC method is presented where the decision to measure a new value of I_{sc} is made on the basis of the current limit.

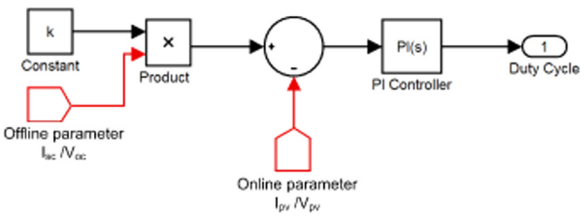

Fig. 4. Block diagram of off-line MPPT method.

3.1.1.2. Fractional open circuit voltage (FOCV) MPPT. In this technique, open circuit voltage is considered as off-line parameter. The I-V curve of the PV module reveals that the voltage at MPP (V_{mpp}) occurs at a fraction of the open circuit voltage V_{oc}. Mathematically, it can be expressed as follows [25,26]:

$$V_{mpp} = k_v V_{oc} \quad (4)$$

The value of k_v is usually between 0.7 and 0.8 and can be calculated using the data sheet of the PV module. As seen in the Eq. (4), this method is also based on approximation. It is best suited for low voltage high current applications [22]. This method has a reasonable tracking accuracy under a steady weather condition. The disadvantage is the periodic power loss due to intermittent measurement of V_{oc} [26]. For large scale use of this method, in [27], authors proposed the use of an unloaded PV module to measure the open circuit voltage.

3.1.2. Hill climbing methods

Three methods are commonly reported in this category i.e., perturb and observe (P&O) or hill climbing (HC), and incremental conductance (Inc). The basic philosophy is same for these methods, however, the algorithm functionality differs for each of them. Note that the only difference between P&O and HC is the perturbation variable. In P&O the voltage or current, while in HC duty cycle (D) is the perturbation variable. InC works on the basis of slope measurement of P-V curve.

3.1.2.1. Perturb and observe (P&O). P&O algorithm compares the power of two points after taking voltage, current, or duty cycle perturbation. In some papers the term hill climbing (HC) is used if the duty cycle is perturbed [28,29]. The basic algorithm is a 2-point power comparison algorithm shown in Fig. 5 [30]. The flowchart working is as follows. The instantaneous PV current I_{pvnew} and voltage V_{pvnew} are measured and multiplied to get the instantaneous power P_{pvnew}. The P_{pvnew} is then compared with the power P_{pvold} that was sampled during the last interval. Next, the decision about the slope of the curve is made by comparing V_{pvnew} with V_{pvold}. Thereafter, the duty

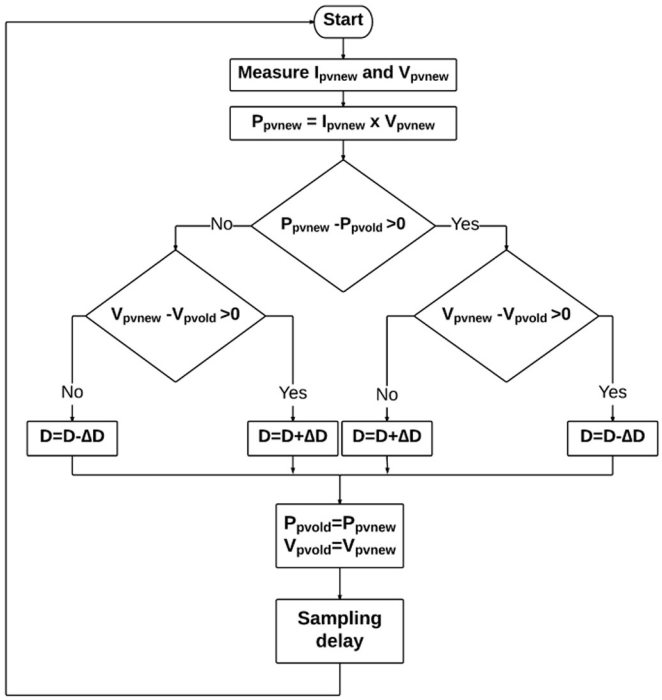

Fig. 5. Flowchart of P&O algorithm with duty cycle control.

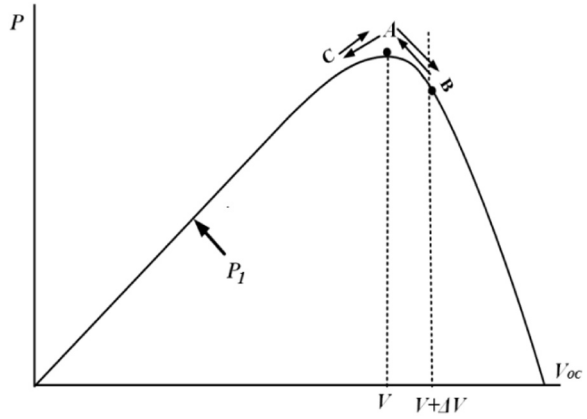

Fig. 6. MPPT oscillating around MPP.

cycle is perturbed and before the end of the sampling instant the V_{pvnew} and P_{pvnew} are stored as P_{pvold} and P_{pvold}. If the perturbation results in power increment then the perturbation is applied again in the same direction otherwise the perturbation is applied in other direction. The flowchart of this algorithm reveals that the perturbation is applied repeatedly during every sampling event and therefore the resultant output power oscillates around MPP as shown in Fig. 6 [31]. The magnitude of this oscillation can be reduced by minimizing the perturbation step size, however; this results in slower tracking speed. Considering a perturbation in the duty ratio, an appropriate step size (ΔD) plays an important role to track the MPP. If the step size (ΔD) is too large, P&O algorithm results in large oscillations about maximum power point. Too small step size results in slow response to changes in irradiance [32].

In general, PV voltage is less sensitive to irradiance, therefore, voltage is regulated by P&O technique through duty cycle of converter [33]. P&O is good for full-sun condition (no partial shading), however, under partial shading condition the algorithm suffers in two ways. Consider Fig. 7, in which local and global MPP are shown. In this condition the conventional P&O algorithms may get trapped and keep on oscillating around the local maxima L_m or L_{m2}, which are lower than the global maximum (GM). It is evident from the Fig. 7 that P&O is not able to distinguish between local maxima and global maxima and therefore, it will not operate at the optimal operating point. Moreover, under rapidly changing environmental conditions, this method may lead the system in wrong direction. Consider Fig. 8 and suppose that the system is operating at point A, suddenly the lighting condition changes and the system moves to point B1. At this point the algorithm checks the power difference which is B1-A $>$ 0. Next the algorithm checks the voltage difference which is B1-A $>$ 0 and therefore, the duty ratio is decreased. This moves the operating point to B2, that is away from the original point B. This phenomenon is called drifting. Furthermore, under low light conditions, the algorithm performance is badly compromised because of the low slope of the power curve. P&O method is extensively used in PV systems due to the following advantages: 1) reasonable dynamic and steady tracking of MPP, 2) analog and digital implementations are possible, 3) low hardware and software complexity, and 4) power is delivered to load during tracking.

Researchers around the world have proposed variations in the conventional algorithm while maintaining the operational principle [36–48]. These variations are made to enhance the MPP tracking speed, to reduce the number of sensors required and power comparison points, and sometimes to replace the sensor positions. In these techniques, the performance of P&O is enhanced by using adaptive perturb value instead of fixed voltage or current perturbation [34,35]. The idea is to use large step size initially, and after reaching the MPP the step size is reduced to compensate the power oscillations [34,35,38,39]. The step size can be made adaptive either by amending the conventional flowchart or by using specialized mathematical functions like 2D gaussian function [49]. Adaptive perturbation is a good choice for normal environmental conditions, however; under drastically changing environmental conditions the drifting problem makes the system moves farther than the MPP. The drifting issue is addressed by [50]. Usually, the conventional hill climbing algorithms require two sensors for power computations, several researchers have developed methods for sensorless computation of either current or voltage thus, resulting in reduced number of sensors [51–55]. The conventional method has sensors installed on the PV side. However, some researchers have proposed the replacement of sensor to the load side [56–59]. In [60], authors proposed a method that uses multi-perturb variables to optimize the power of PV module.

The conventional method compares the power before and after perturbation, and it is, therefore, a 2-point power comparison method. Several researchers have reported more than 2 power comparison points that resulted in correct tracking under rapidly changing environmental condition [61]. MPPT [62] has presented an improvement for both P &O and InC such that the power measurement between two perturbations is computed numerically and therefore it is a 3-point power comparison. In order to tackle the issue of partial shading, MPPT [63] proposes an improvement that they call checking algorithm. The checking algorithm stores the initial operating point using the conventional P&O method and then shifts to checking algorithm that decides about checking the new operating point on the curve. The checking algorithm actually hunts for the next operating point and compares the power between the last saved power and the new power. Then it stores the new values and again hunts for some other operating

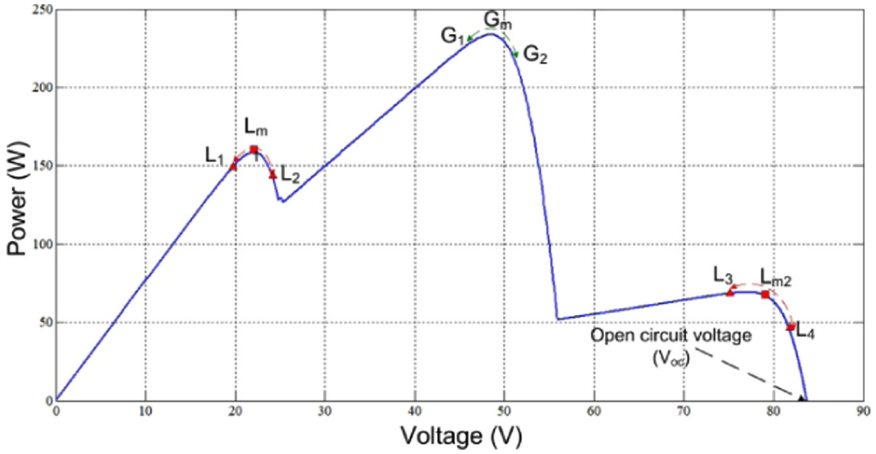

Fig. 7. Partial Shading case.

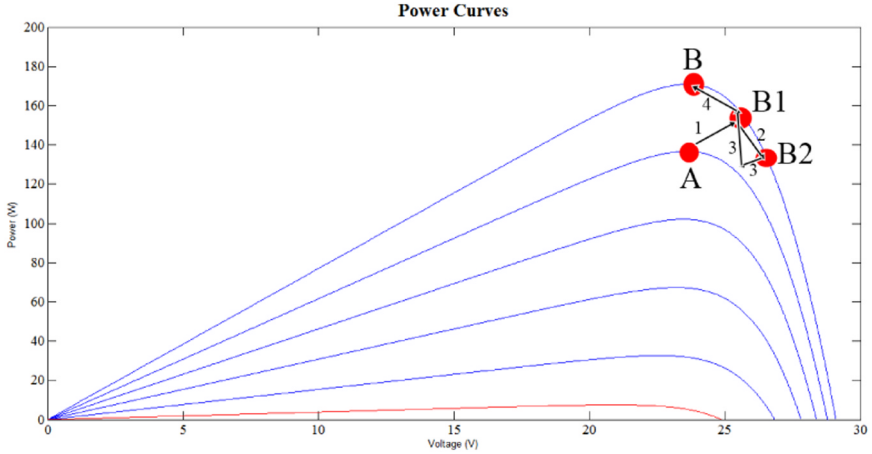

Fig. 8. Performance of P&O.

points. It then establishes from the stored data about the exact operating point. Hence, it is also a multiple comparison point. Note that partial shading MPPTs are reviewed in a separate section. However, since MPPTs [63-6] are off-shoots of conventional methods, they are discussed here. The work presented by [64] works on the comparison of three points where the additional measurement point is in between the first and second perturbation. MPPT [65] is an improvement in P&O method to track the GM using a mechanism that confines the voltage range between the closely located peaks only. Methods [66,67] provide a modification in P&O and InC respectively with three operating points, the resultant MPPT is self predictive.

3.1.2.2. Incremental conductance (InC) MPPT. The InC algorithm tracks the MPP by using the information about the slope of the power curve. MPP is said to be achieved when the slope of the power or the derivative of the PV array power (dP/dV) is zero. Fig. 9 reveals that the derivative of power is positive if operating point appears on the left of MPP. If operating point appears on the right of MPP, the derivative is negative [68]. The technique tends to make the slope zero by varying the operating point. However, the MPP tracking speed reduces in rapidly changing environmental conditions because of the continuous change in the power curve slope. The algorithm operating rules for positive, negative and zero slopes are explained in Eqs. (5)–(13).

$$\frac{dP}{dV} = 0 : \textit{If operating point is on MPP} \tag{5}$$

$$\frac{dP}{dV} > 0 : \textit{If operating point is on left of MPP} \tag{6}$$

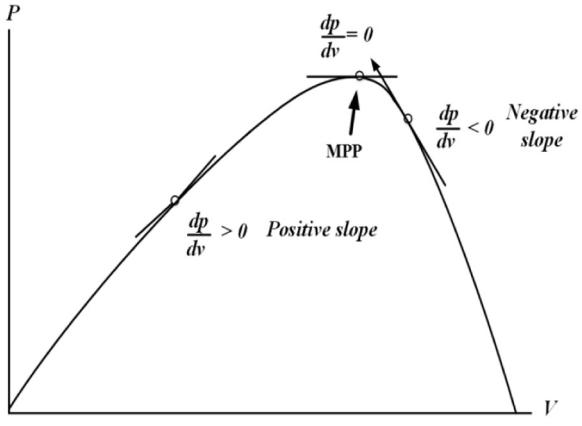

Fig. 9. Arbitrary P-V curve to demonstrate the concept of slope.

$$\frac{dP}{dV} < 0 : \textit{If operating point is on right of MPP} \tag{7}$$

For MPP,

$$\frac{d(VI)}{dV} = 0 \tag{8}$$

$$I + V\frac{dI}{dV} = 0 \tag{9}$$

$$I + V\frac{\Delta I}{\Delta V} = 0 \tag{10}$$

$$\frac{\Delta I}{\Delta V} = -\frac{I}{V} : \textit{If operating point is on MPP} \tag{11}$$

$$\frac{\Delta I}{\Delta V} > -\frac{I}{V} > 0 \quad : \textit{If operating point is on left of MPP} \tag{12}$$

$$\frac{\Delta I}{\Delta V} < -\frac{I}{V} < 0 : \textit{If operating point is on right of MPP} \tag{13}$$

In pursuit of MPP, the controller makes the comparison between I/V and $\Delta I/\Delta V$ and the PV array is settled at reference voltage (V_{ref}) as shown in Fig. 10. If the difference exists then the operating point is adjusted to make the slope zero. The system halts once the operating point is reached, based on two conditions. First, if the stored values of current and voltage become equal to the previously stored value, second, if the ratio of rate of change of voltage with the rate of change of current equals the conductance (I/V). The InC algorithm adjusts the operating voltage of PV array to satisfy the condition of Eq. (11). Once the MPP is achieved, the algorithm sets the PV array at this MPP point. The capability of stopping at MPP makes this method superior than P&O. Nevertheless, the MPP tracking speed and accuracy depend on the increment size. The bigger increment size can track the MPP at faster rate but it may cause oscillations around MPP. This algorithm involves high sampling rate and fast computations for power slope. Sensors measure instantaneous voltage and current and a simple micro-controller maintains record of past values of V and I for making decision. InC is a prominent MPPT algorithm due to its following salient features:

1) true MPPT technique, 2) low hardware complexity, 3) reasonable convergence speed, 4) negligible oscillations around MPP, 5) stops at MPP when slope becomes zero, and 6) only V and I sensors are needed. However, the traditional InC technique is complex regarding software implementation and does not track global peak under PS conditions. As shown in Fig. 10, in case of multiple peaks in a P-V curve there is no provision of detecting a global maximum and therefore, similar problems viz PS occur in InC as discussed in P&O method.

To overcome these drawbacks, following improved versions of InC algorithm have been proposed by various researchers. The modified InC

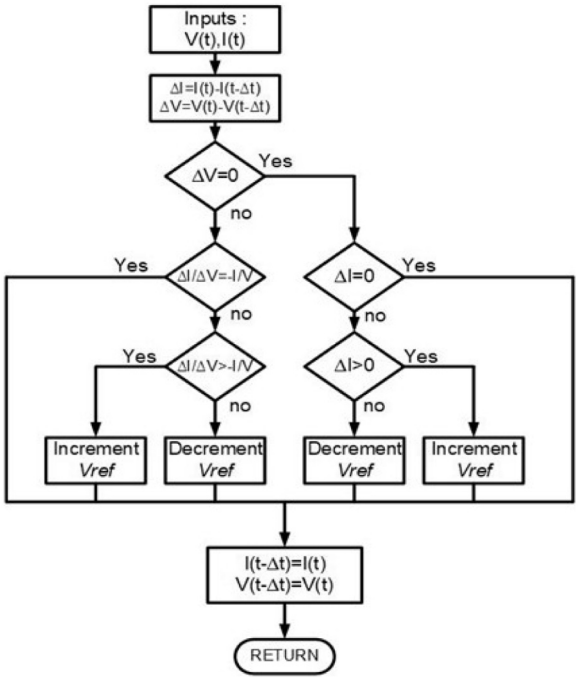

Fig. 10. Flowchart of InC algorithm [68].

algorithm, proposed by [69,70], finds global maximum under partial shading conditions. In these methods, multi duty cycle control of converter is involved, which obtains multiple peaks using periodic characteristics of P-V curve. This algorithm separates the local maxima and global maximum of these peaks.

Variable step size InC implements the automatic tuning control of step size for the MPP operation under both steady state and dynamic conditions [41,71]. This technique mitigates oscillations around MPP and improves tracking position under steady state. However, under abrupt weather conditions the phenomenon of drifting is observed. The working of this scheme is explained by Eq. (14):

$$D(k) = D(k-1) \pm N\left[\frac{P(k) - P(k-1)}{V(k) - V(k-1)}\right] \tag{14}$$

where *D(k)* is instantaneous duty cycle, *P(k)* is instantaneous power and *V(k)* is instantaneous voltage. *D(k-1)*, *P(k-1)* and *V(k-1)* are previous duty cycle, power and voltage respectively. *N* is scaling factor which varies between 0.06 and 0.12 to regulate the step size.

An improvement in variable step size InC is proposed in [72], where variable step size and incremental resistance are combined together to operate PV array at MPP. The advantages of this method include: 1) fast convergence to MPP, and 2) simple and accurate MPPT. The threshold function *C* used to switch various step size modes is given by Eq. (15):

$$C = P^n\left(\frac{dP}{dI}\right) \tag{15}$$

where *n* represents an index, P^n is output power of PV array and *dP/dI* is derivative of power with respect to current. This technique operates in fixed as well as variable step size modes as stated below:

$$\frac{\Delta C}{\Delta I} \geq 0\text{: Left of MPP - Step size mode is fixed variabe} \tag{16}$$

$$\frac{\Delta C}{\Delta I} < 0\text{: Left of MPP} - \text{Step size mode is variable} \tag{17}$$

$$\frac{\Delta C}{\Delta I} > 0\text{: Right of MPP} - \text{Step size mode isvariable} \tag{18}$$

In [73], a power increment based IC algorithm is proposed, which uses the reference point with the following two controls and one tracking zone:

- Control of variable frequency through constant duty cycle
- Control of constant frequency with variable duty cycle
- Zone of threshold tracking (TTZ)

The MPP is tracked in both sides of PV curve using TTZ. The TTZ is divided into two segments: 1) zone of conductance threshold (CTZ), and 2) zone of power threshold (PTZ). The conductance increment (ΔC) measured for CTZ and power increment measured for PTZ are given by Eq. (19) & (20) respectively:

$$-\rho 1\frac{I_{PV}}{V_{PV}} > \Delta C > -\rho 2\frac{I_{PV}}{V_{PV}} \tag{19}$$

$$P\rho_1 > \Delta P > P\rho_2 \tag{20}$$

When MPP tracking is done inside TTZ, then the primary measure is ΔC. The primary measure becomes ΔP if tracking is done outside the TTZ.

3.1.3. MPPTs inspired from PV behavior and intelligence methods

A ripple correlation method is presented in [74]. This method is based on estimating the ripple of the dc link. For example, an MPPT realized by a dc-dc converter has ripples in the dc link as a result of the switching action. These ripples are used to find MPP of PV array [74]. As ripples are generated automatically while switching the converter, so no artificial perturbation is needed. This concept takes on the derivative of the power and voltage. Later, it is estimated if the derivative product is positive, negative or zero. This is used to establish the status of the gradient. If it is zero then the MPP is reached. RCC based methods are mostly implemented using the current as a reference value because the voltage across inductor provides information about the derivative of the current. RCC can be implemented either through analog or digital circuitry [75,76].

RCC correlates *dP/dt* with either *dV/dt or di/dt* to force the ripple of power to be zero, thus reaching the MPP.

a) If $dV/dt > 0$ or $di/dt > 0$ and $dP/dt > 0$, it means the MPP is above the operating point. In this case, $V < V_{mpp}$ or $I < I_{mpp}$
b) If $dV/dt > 0$ or $di/dt > 0$ and $dP/dt < 0$, it means the MPP is below the operating point. In this case, $V > V_{mpp}$ or $I < I_{mpp}$
c) If $dV/dt = 0$ or $di/dt = 0$ and $dP/dt = 0$, it means the MPP is at the operating point. In this case, $V = V_{mpp}$ or $I = I_{mpp}$

RCC method can be used for any power converter topology to maximize power of PV array. When boost converter topology is used, increase in duty cycle increases the inductor current i_L which is equal to PV array current and PV array voltage decreases. Therefore, duty ratio (*d*) of converter is control input which is calculated using following expression:

$$d = K\int \frac{d_{ij}}{d_t}\frac{dP}{dt}dt \tag{21}$$

The RCC method is simple, less expensive, quick and true MPP tracking technique under varying irradiance levels.

The technique [77] uses current sweep waveform for PV array to obtain and update the I-V characteristic at fixed time period. The V_{mpp} is then measured from I-V curve at the same time period. The current sweep function is sated in Eq. (22):

$$(t) = k\frac{di}{dt} \tag{22}$$

where *k* is constant of proportionality. The power *P(t)* obtained from PV array is given as:

$$P(t) = v(t)i(t) \tag{23}$$

At MPP, slope of power or derivative of power with respect to '*t*' becomes zero. Therefore:

$$\frac{dP(t)}{dt} = \frac{d\ [v(t)i(t)]}{dt} = 0 \tag{24}$$

$$\frac{d\ [v(t)i(t)]}{dt} = 0 \tag{25}$$

$$i(t)\frac{dV(t)}{dt} + v(t)\frac{di(t)}{dt} = 0 \tag{26}$$

Putting value of *i(t)* from Eq. (22) in eq. (66):

$$\frac{dP(t)}{dt} = k\frac{di(t)}{dt}\frac{dV(t)}{dt} + v(t)\frac{di(t)}{dt} = 0 \tag{27}$$

$$\frac{dP(t)}{dt} = \left[k\frac{dV(t)}{dt} + v(t)\right]\frac{di(t)}{dt} = 0 \tag{28}$$

This can be simplified as

$$\frac{dP(t)}{dt} = \left[k\frac{dV(t)}{dt} + v(t)\right] = 0 \tag{29}$$

Current sweep MPPT technique involves analog computations to compute V_{mpp}. Eq. (29) is used to confirm whether the MPP has reached. The reference point is continuously updated to obtain MPP.

Forced oscillation based MPPT injects a sinusoid perturbation into the switching frequency and compares it with PV array output voltage as shown in Fig. 11 [78,79]. The input voltage V_{pv} is sensed on varying the switching frequency. After comparing the values of βV_{pv} and reference voltage V_{ref}, the duty cycle of the power converter (dc-dc) is set at MPP. Once the MPP is obtained, the intermediate parameter β should be constant. The value of β is calculated as in Eq. 30(30)

$$\beta = ln\left[I_{pv}/V_{pv}\right] - C^{*}V_{pv} \tag{30}$$

where $C = \frac{q}{AKTN}$, q is electron charge, A being the ideality factor of diode, K represents the boltzmann constant, T is absolute temperature, and N is the number of series connected cells.

A curve fitting based technique [80] uses a 3rd order polynomial function, as given in Eq. (31), to extract MPP from PV array:

$$P = aV^3 + bV^2 + cV + d \tag{31}$$

PV array voltage and power is sampled in intervals to determine *a*, *b*, *c* and *d* coefficients. At MPP, $dP/dV = 0$:

$$\frac{d}{dV}(aV^3 + bV^2 + cV + d) = 0 \tag{32}$$

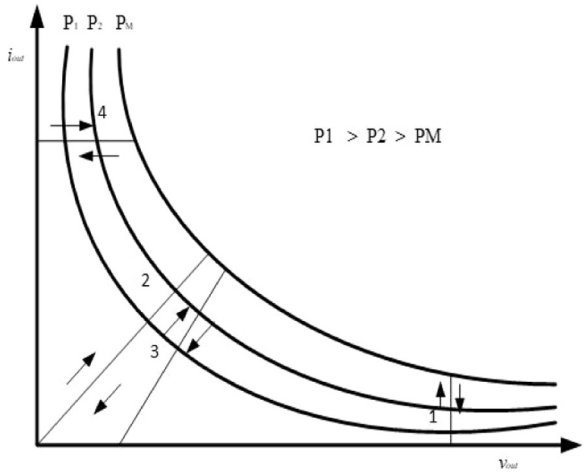

Fig. 12. Various loads connected to PV array [56].

$$3aV^2 + 2b\,V + c = 0 \tag{33}$$

Voltage corresponding to MPP is calculated using the following expression:

$$V_{mpp} = \frac{-b \pm \sqrt{b^2-3ac}}{3a} \tag{34}$$

The coefficients *a*, *b* and *c* are constantly sampled in intervals of milliseconds to calculate V_{mpp}. Some varients of this method are given in [81–83].

One cycle control (OCC) technique comprises of single-stage inverter [84–86], where the MPP is attained by adjusting the output current (I_{out}) of converter with reference to output voltage of PV array. MPPT based on load current/voltage maximization is presented in [56]. A lossless converter configured between PV array and load, boosts both the output powers of PV array and converter load. Similarly, enhancing the power of the converter load enhances the power of the PV array [56]. Fig. 12 depicts that the practical loads connected to PV array may be individual or combination of resistive source, voltage source and current source [56]. Fig. 12 yields the following facts: a) a load of voltage source maximizes the ouput current (i_{out}) to extract MPP, b) a load of current source boosts the ouput voltage (v_{out}) to reach MPP, and c) for rest of loads, either i_{out} or v_{out} should be maximized to track MPP [56]. As lossless converter is assumed in this technique, exact MPP is almost never achieved.

A linear current control (LCC) method [36,87] is based on the linear

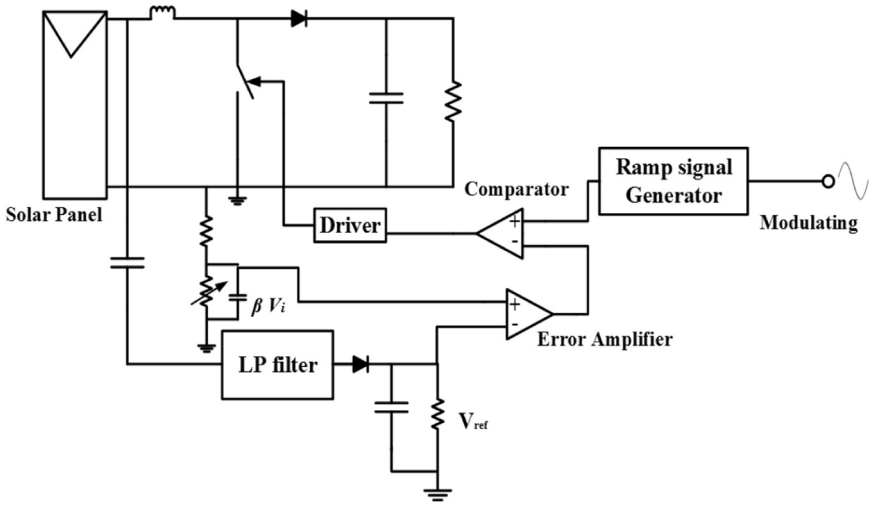

Fig. 11. Implementation of Forced oscillation based MPPT [78].

relationship between irradiance and PV current. At higher irradiance level, the PV current almost exhibits linearity with voltage due to series resistance of PV array. This linearity helps in tracking the MPP using a set of linear equations. Once I_{mpp} and V_{mpp} are computed using linear equations, the PI controller and feedback system operate PV array at MPP. The drawback of this technique involves hardware and software complexity.

In best fixed voltage (BFV), the irradiance and temperature samples are gathered for long period and BFV is found. The algorithm adjusts array's operating point to BFV. Otherwise, it adjusts the output voltage to load voltage [88,89]. In temperature control method [90,91], temperature sensors and temperature function are used to trace MPP, since PV array power is temperature and irradiance dependent. The implementation of TM is simple and cost effective and has excellent tracking factor [92]. The extremum seeking control (ESC) technique involves Lyapunv function to map non-linear input-output of PV system to extract MPP [93,94]. This reduces the perturbations around MPP and hence this technique has fewer oscillations in MPPT. An adaptive ESC further improves the efficiency of MPPT [94]. In TEODI approach technique, two identical PV systems are used to equalize the output operating points through forced displacement of input operating points [95–98]. Fig. 13 depicts the implementation of teodi [96]. The overall configuration resembles a micro-converter (dedicated dc-dc converter for each panel), however, the output current and voltage of each dc-dc converter is sensed, compared and thereafter, the control process is centralized. However, the PV panels are operated separately to match the output current and voltage. The teodi approach offers the following advantages: 1) analog implementation is effective and cheap, and 2) less sensitive to irradiance variations and noise of converter. However, this technique does not work properly if mismatching occurs between two PV modules/arrays.

The variable inductance based MPPT uses variable inductor in dc-dc buck converter to operate PV array at MPP. The researcher [99] proved the robustness and reliability of this technique by experimental results under varying weather conditions. In case of lower irradiance, higher value of inductance is adjusted, while lower value of inductance is selected in case of higher irradiance. The lower limit of inductance to extract maximum power from PV array is given by Eq. (35).

$$L_{min} = \frac{D^2(1-D)V_{pv}}{2 \quad f_s I_{pv}} \tag{35}$$

The overall size of inductor can be reduced by 75% using variable inductor and the value of inductor can be varied in accordance with the irradiance levels. This method can be applied to any basic dc-dc converter.

Bisect search theorem (BST) [100] is a mathematical technique to find the roots of any function $y = f(x)$ in an interval [a,b]. The function depends on x and contains a root x^*. When applied to a PV system, the function will be $\Delta P/\Delta V$ and the interval will be $[0,V_{oc}]$.The root V_{mpp} lies

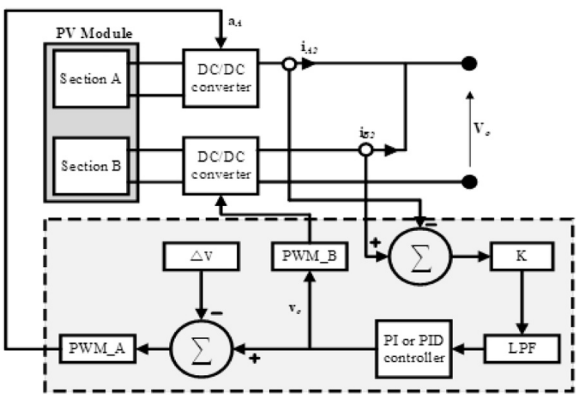

Fig. 13. Teodi MPPT controller [95].

between the interval 0 and V_{oc}. The function becomes zero at MPP. This method is simple in hardware implementation and cost effective as it requires less sensors.

3.1.4. Hybrid MPPTs

The MPPT methods discussed above can be combined together to form a hybrid MPPT [101–120]. It usually attempts in gaining the advantages of the fused methods while discarding their disadvantages. The resultant hybrid MPPT can be an off-line method or an on-line method. An off-line hybrid MPPT is formed if the combined MPPTs are both off-line or if an off-line MPPT is combined with an on-line MPPT. The combination of two on-line methods yields a resultant on-line hybrid method.

3.1.4.1. Off-line hybrid MPPT. One combination is to combine the basic offline methods i.e., FSCC and FOCV [101]. Another aspect is to combine the off-line methods with hill climbing algorithms [106–109]. Some authors have combined three methods to track the MPPT e.g., in [113] the MPPT measures I_{sc} and V_{oc} and then approximated MPP is calculated using the diode ideality constant and reverse saturation current. It then shifts to the P&O method to track the actual MPP.

3.1.4.2. On-line hybrid MPPT. The on-line hybrid MPPT methods can be designed in a variety of ways. One way is to combine the conventional on-line methods with modifications to cater for the deficiencies of conventional methods [114]. The main task is either to combine the advantages or to diminish the inherent deficiencies. For example, the drifting of P&O is eliminated using FLC in [116].

3.1.5. Ranking of full-sun MPPT methods

The ranking of MPPT methods that work under full-sun conditions is mentioned in Table 2. The values of AC, Him TS, and SS-E for each MPPT are entered in accordance with the criterion developed in Section 2 and Table 1. The overall rating of each MPPT is formulated with regard to Eq. (1). Besides that the search variable, converter used, and load application -are also mentioned.

3.2. Partial shading MPPTs

In this section, MPPTs specially designed for partial shading conditions are discussed in comprehensive manner with special focus on I-V curve tracer, restricted voltage window and bio-inspired MPPTs.

3.2.1. I-V curve tracing MPPTs (I-V tracer)

The MPPTs from this category utilize the transient evolution of capacitor to trace the power-voltage (P-V) characteristics of a photovoltaic (PV) array [121,122]. In general, MPPTs work in association with dc-dc converter, which is installed between PV array and load as shown in Fig. 14(a). The duty cycle (D) of the converter is served as a search variable for MPPTs. For each perturbation in D, converter requires a settling time in the range of 5–50 ms as shown in Fig. 14(b). It is because of the well-known second order transients of the converter [123]. At times, several adjustments in D are required to fix the PV array at a specific point. In the search of global maximum (GM), MPPT examines numerous points on P-V curve, which makes the tracking time of these methods in hundreds of milliseconds, if not in seconds. Note that during GM searching, PV array is not operated at maximum power during the search. The mathematical principle of MPPTs [121,122] that rely on 1st order transients of capacitor (C_{scan}) for fast scanning of P-V curve is presented in (36):

$$\Delta v_{PV} = \Delta v_C = \frac{I_{pv}}{C_{scan}} \Delta t \tag{36}$$

The implementation of these methods requires a modification in the conventional circuit, which is shown in the form of black dotted lines in

Table 2
Criterion to determine the ranking of MPPTs.

MPPT	Classification	Algorithm's Complexity (1–5) in accordance with Section 2.1	Hardware Implementation (1–5) in accordance with Section 2.2	Tracking Speed (1–3) in accordance with Section 2.3	Steady-state efficiency for uniform condition (1–3)in accordance with Section 2.4	Overall Rating according to Eq. (1)	Search/ Control Variable	Converter	Load Application
Fractional MPPT (FSCC-FOCV) [22]	Fractional MPPT	1	3	2	3	2.33	Duty	Buck-Boost	Resistive
FSCC [24]	Fractional MPPT	1	4	2	3	2.5	Duty	Boost	Resistive
Adaptive P&O [57]	Adaptive Hill Climbing	3	2	2	1	1.83	Duty	Buck	Resistive/ Battery
InC [41]	Adaptive Hill Climbing	4	1	2	1	1.83	Voltage	Boost	–
InC [70]	Modified Hill Climbing	4	1	2	1	1.83	Duty	SEPIC	Resistive
RCC [75]	PV behavior MPPTs	3	2	2	1	1.83	Voltage	Boost	Grid
Forced oscillation [78]	PV behavior MPPTs	2	4	2	1	2	Voltage	SEPIC or Cuk	Resitive
Curve Fitting [82]	PV behavior MPPTs	3	3	2	1	2	Duty	Boost	Resistive
OCC [117]	PV behavior MPPTs	3	3	2	1	2	Voltage	Inverter	Grid
Load V or I maximization [56]	PV behavior MPPTs	3	3	2	1	2	Duty	Synchronous Buck	Resistive
Linear current control [36]	PV behavior MPPTs	3	3	2	1	2	Duty	Boost	Resistive
BFV [88]	PV behavior MPPTs	3	2	2	2	2.17	Duty	Buck	Motor
TM [91]	PV behavior MPPTs	2	3	2	2	2.17	Voltage	Boost	Resistive
ECS [94]	PV behavior MPPTs	4	2	2	1	2	Current	Boost	Battery
TEODI [97]	PV behavior MPPTs	2	4	2	1	2	Voltage	Boost	Battery
Variable inductor [99]	PV behavior MPPTs	2	2	2	2	2	Duty	Buck	Resistive
BST [100]	PV behavior MPPTs	3	1	2	2	2	Duty	Boost	Resistive
Hybrid method [109]	PV behavior MPPTs	3	2	2	1	1.83	Duty	Boost	Resistive and Battery

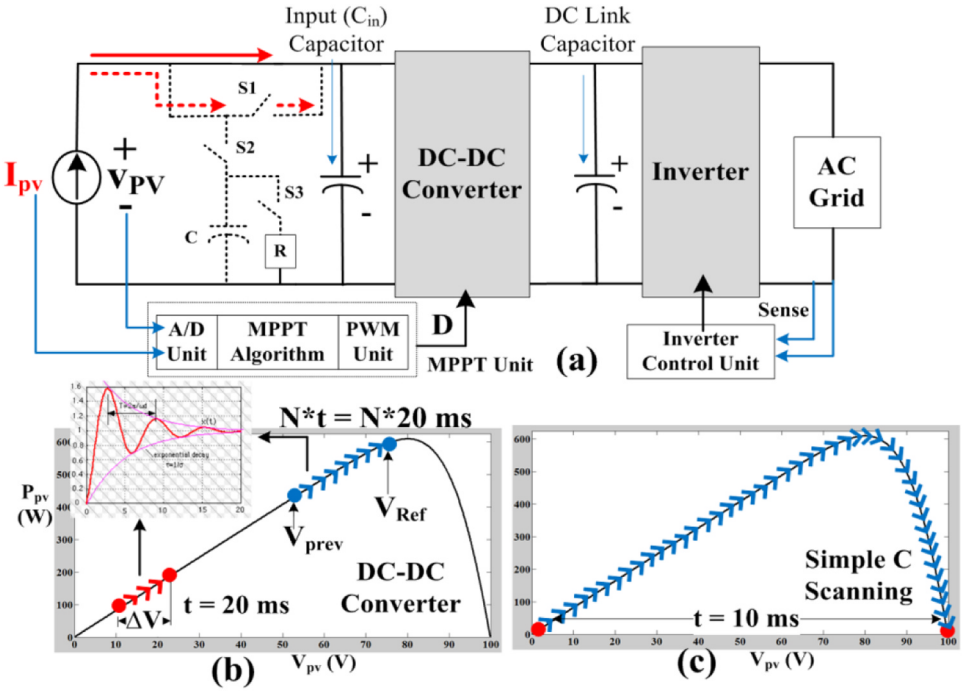

Fig. 14. (a) Extra circuit (circuit in dotted lines) for I-V tracer, (b) Execution of MPPT through dc-dc converter, (c) P-V curve tracing with capacitor [127].

Fig. 14(a) [121]. Utilizing inherent features of capacitor, the P-V curve can be scanned in tens of milliseconds. This duration is almost equivalent to the execution time of single voltage step of other MPPTs as evident in Fig. 14(b) & (c). Consequently, capacitor scanning based MPPT has fast convergence speed and better dynamic efficiency. These methods have following advantages:

- These methods do not suffer from second order transients of dc-dc converter during scanning of PV curve, since they utilize first order transient evolution of capacitor.
- Contrary to traditional MPPTs, which employ a complex and time taking tracing method, these methods are simple, fast, and inexpensive. Moreover, they can be expanded to any array size.

The work presented in [122] has theoretically estimated the relationship between C_{scan} and total scanning time (t_f) on the basis of size of PV array as represented in Eq. (37). Whereas, the experimental validation of this C_{scan} formula is presented in [121].

$$C_{scan} \cong 0.55 \times \frac{I_{sc,m} \times N_p}{V_{oc,m} \times N_s} \times t_f \tag{37}$$

where N_p and N_S represent number of modules in parallel and series, respectively. While, $I_{sc,m}$ symbolizes short-circuit current and $V_{oc,m}$ stands for open-circuit voltage of the module.

However, these methods suffer from following drawbacks:

- In order to scan the P-V curve with parallel capacitor [121,122], PV array is isolated from load, which results in power unavailability at load during scanning time.
- To re-initialize every succeeding scanning, it is necessary to dissipate the previously stored energy in capacitor through an external resistor, which results in further power losses [121].

Keeping in view the aforementioned disadvantages, the methods presented in [124–126] perform the scanning of I-V curve through dc-dc converter. The working principle of these methods involve in setting the D of converter at one extreme, and then to other extreme. In the process, the P-V curve is traced and information of GM is stored. After that, the D is re-modulated at the GM point. Consider that D is set at 0.7 and PV array is operating at GM. Whenever weather condition changes, these techniques set the D from 0.7 to 1 and then from 1 to 0. In this way, P-V curve is scanned from short-circuit voltage to open-circuit voltage of array. The drawback of these methods are:

- Since these methods use the input capacitor (C_{in}) of converter instead of separate capacitor, these methods may have compatibility and scalability issues with PV arrays having small C_{in}. Moreover, an A/D converter with fast sampling rate is required.
- These MPPTs consume extra time to set the converter at one extreme before initializing the scanning.
- These methods also exhibit momentarily power cut-off to load because of extreme converter operation.

In [127], a new MPPT technique is proposed which scans the P-V curve of PV array with a series capacitor (C_{scan}) through a unique H-bridge architecture as shown in Fig. 15(a). The proposed technique employs a simple algorithm which controls H-bridge to scan the P-V curve in two sequences: 1) during charging of capacitor, and 2) during discharging of capacitor. The proposed MPPT neither requires the isolation of PV array from load nor does it result in power loss during scanning of P-V curve. In this paper, the comprehensive discussion regarding the effects of input capacitor (C_{in}) of converter during scanning of P-V curve is presented. Also, sizing of capacitor C_{scan} according to array size is explained with a design example. The working principle of the proposed method is as follows:

Sequence – 1 (Capacitor charging sequence): In start, V_{pv} of array is organized at $0.1V_{oc}$. Then switches S2 and S4

are closed. Consequently, the capacitor (C_{scan}) is hooked up in a polarity that is opposite to PV array, as shown in Fig. 15(b). The mathematical expression of such circuit is expressed as:

$$v_{PV}(t)\uparrow - v_C(t)\uparrow = 0.1V_{oc} \tag{38}$$

Since $v_C = 0$ at t = 0, PV array starts operating at $0.1V_{oc}$ as indicated in the above expression. With the passage of

time, the capacitor will charge with I_{pv} of array and its voltage v_C rises from zero. This in turn, causes v_{PV} to rise, as

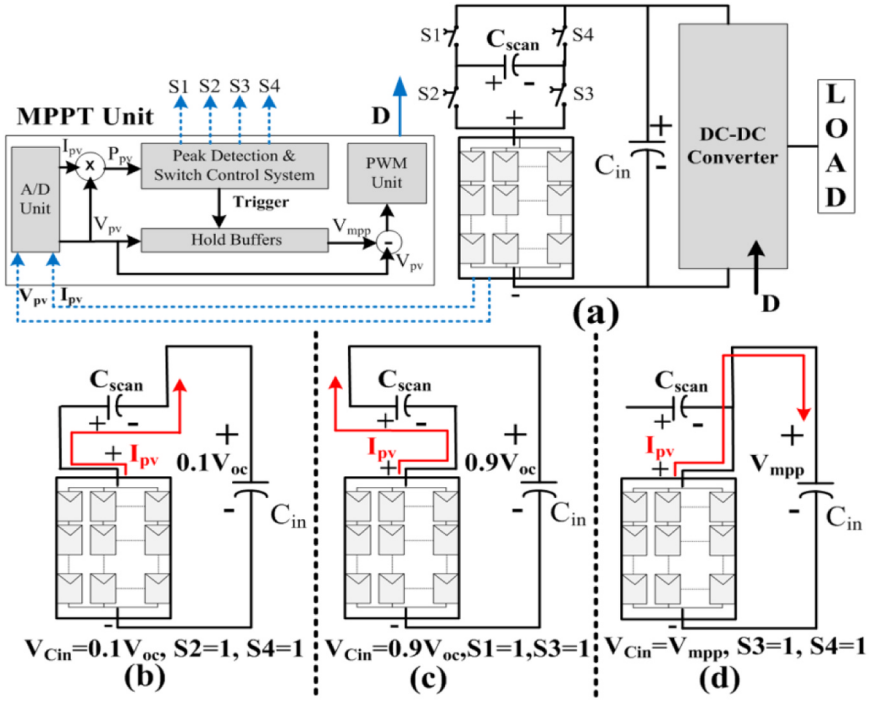

Fig. 15. (a) A series capacitor tracer MPPT with H-bridge architecture, (b) organization of circuit when switches S2 and S4 are on, (c) organization of circuit with S1 and S3 are on, (d) bypassing of C_{scan} with S1 and S2 are on [127].

the difference between v_{PV} and v_C is equal to the fixed output voltage of $0.1V_{oc}$ as expressed in Eq. (38). Finally, when v_{PV} becomes equal to V_{oc}, v_C reaches $0.9V_{oc}$. In this way, P-V curve is traced from $0.1V_{oc}$ to V_{oc}.

Sequence – 2 (Capacitor discharging sequence): During this sequence, PV array is set at $0.9V_{oc}$ and switches S1 and S3 are turned on. The circuit transforms into a configuration where both PV array and capacitor (C_{scan}) are connected in series with the same polarity as shown in Fig. 15(c). This can be mathematically expressed as:

$$v_{PV}(t)\uparrow + v_C(t)\downarrow = 0.9V_{oc} \tag{39}$$

It is to be noted that C_{scan} is already charged to $0.9V_{oc}$ during the previous iteration in Sequence-1. Since the output voltage is fixed at $0.9V_{oc}$ and v_{PV} is zero at t = 0 as depicted by Eq. (39). Gradually, the capacitor starts discharging at the rate determined by I_{pv} of array. As a result, v_C of C_{scan} falls while v_{PV} of array rises as indicated by Eq. (39). This process continues until C_{scan} becomes completely discharged. At this point, v_{PV} becomes equal to $0.9V_{oc}$ and P-V curve is scanned from 0 to $0.9V_{oc}$. Note that energy stored in C_{scan} during the previous scanning is re-injected into load during the current scanning. Consequently, no energy is dissipated or lost.

The main disadvantages of this method are:

- Extra hardware in the form of H-bridge is required
- During each scanning, the algorithm requires extra step to set the PV array at $10\%V_{oc}$ or $90\%V_{oc}$, thus fast converter with low settling time is required.

3.2.2. Restricted voltage window MPPTs (voltage zones)

The MPPTs from this category are developed after extensive probing of P-V/I-V characteristics of array through theoretical analysis, mathematical modeling, and practical results [128]. A common consensus between scientists is existed that voltage regions in which local maximum (LM) or global maximum (GM) may appear are equal to number of series connected modules (N_s) in a PV array [19]. The partitioning of these regions depend on the integral multiples of open-circuit voltage (V_{oc}) of the module. Therefore, the objective mission of these MPPTs revolves around following major challenges:

- Acquiring the ability to distinguish between uniform and partial shading (PS) conditions:
  - o In case of uniform condition, transferring of PV array in MPP vicinity and quickly tracks the optimal point
  - o In case of partial shading, obtaining the global maximum (GM) through evaluation of least amount of voltage regions
- Estimation of open-circuit voltage and short-circuit current through sensor-less mechanism or feasible solution.
- Shrinking or expanding of voltage regions because of severe temperature change, and therefore selection of representative point in a region

The principle operation of MPPT presented in [128] checks the power of integral multiples of $0.8V_{oc}$ of each region.

The region which represents the maximum power is declared as global maximum region and PV array is set at that region. After that P& O is applied to track MPP accurately. On similar lines, technique [129] examines the power of mid-point of regions but with intelligent mechnism to restrict the complete scanning of P-V curve. It first estimates the open-circuit voltage of array and then calculates the voltage limit (V_{Lim}) i.e. mid-point voltage of last region as represented in Eq. (40):

$$V_{Lim} = \frac{V_{oc}}{2} + (N_s - 1)V_{oc} \tag{40}$$

This MPPT [129] starts scaning the regions of P-V curve from I_{sc} point. After evaluating power of a region, the technique estimates the power limit (P_{Lim}) by the product of I_{pv} of present region with V_{Lim} calculated from Eq. (40). If P_{Lim} is greater than power of present region, the technique proceeds to examine the next region, otherwise it terminates scanning process. Note that while moving from I_{sc} to V_{oc}, the I_{pv} of array always falls. In this way, the number of voltage regions to be scanned are reduced. The capabilty of this MPPT can be enhanced by restricting the I-V curve further. Another drawback of this method is the estimation of open-circuit voltage of array by isolating the array. In

MPPT [130], the reference voltage is set based on the formula represented in Eq. (41):

$$V_{ref} = \left(1 - \frac{N_s - \sum M_j}{N_s}\right) \times 0.85 \times V_{oc} \quad (41)$$

where, *Mj* is calculated by counting the number of bypass modules at iteration *j*. Here, *j* represents the number of possible irradiance conditions on a PV array. In start, this method scans the I-V curve from right-most region and applies P&O to reach MPP. After that, the other regions of I-V curve are scanned based on sophistication mechnism, the mathematical representation of which is shown in Eq. (41). This method is technically correct and maintains good accuracy under different shading patterns. However, this method requires voltage sensing of each module, which is expensive. Moreover, the application of P&O in each region makes the dynamic efficiency of this method slow.

Keeping in view the high cost of analog sensing of each module, the authors of [131,132] developed efficient MPPTs based on voltage (V_{pv}) and current (I_{pv}) sensing of array. Likewise MPPT [130], the technique [132] starts its operation from right-most region and detects the first peak through P&O. It stops the scanning process if practical power of current region is more than the theoretical power of next region. The theoretical power is estimated through maximum power current of STC (I_{mpp_STC}) and voltage of the future region (V_{Future}), where, V_{Future} is estimated through V_{oc} of module. Due to probabilistic estimation of theoretical power through I_{mpp_STC}, this MPPT cannot smartly skip the in-between regions. It also struggles if two respective peaks in the P-V curve are quite distant from each other.

A global MPPT based on voltage window search (VWS) is presented in [133]. At any operating voltage, power is assessed first. If present power ($P_{present}$) is greater than the stored power, new voltage point (V_{pv_new}) is estimated through $P_{present}/I_{present}$. In this way, the voltage window is restricted between V_{pv_new} and maximum voltage point (V_{pv_Max}). In case, if $P_{present}$ is smaller, a voltage step is induced. To further restrict the voltage regions, technique [134] has designed two voltage phases: downward and upward. In this method [134], the scientific philosophy of technique [132] and VWS [133] is employed in downward voltage and upward voltage phases, respectively.

In another MPPT [135], the voltage regions are assessed based on the integral multiples of open-circuit voltage of module (V_{oc}). Before invoking the hill-climbing (HC) algorithm to detect the GM precisely, the number of bends (peaks) are estimated on I-V curve based on formula presented in Eq. (42). Because of its intelligent way of identifying the GM and better employment of HC, this method is accurate. However, for fast varying partial shading conditions i.e. cloud passing, the dynamic efficiency of this method becomes low.

$$\frac{I_{pv\_prev} - I_{pv\_new}}{I_{pv\_prev}} \leq 0.1 \quad (42)$$

Similar to [129], I_{pv} of constant current region (I_{pv_CCR}) of each voltage region is assessed in MPPT [136] and maximum power of each region is estimated through $0.9I_{pv\_CCR}$. The voltage of each region is based on integral multiples of V_{oc} of module. After identifying the maximum power region, incremental conductance (IC) method is used to reach the GM precisely. In another recent MPPT [137], control algorithm examines the power slope of each region to identify GM, where the distance between regions is equivalent to V_{oc} of module. The main drawback of methods [136,137] is that they cannot differentiate conveniently between uniform and partial shading conditions.

In MPPT [138], a three point sample is taken on P-V curve. The first sample is taken automatically due to occurance of partial shading condition. The second sample is taken at open-circuit voltage of array i.e. upper bound of I-V curve. The third sample is the only one, which is perturbed to reach the lower bound of I-V curve. Next, several samples of I-V curve are taken and maximum power is filtered out (P_{Max}). The distance between samples are considered as voltage regions, where region with maximum power amongst all the regions is further examined. The technique [138] is quite effective under partial shading conditions and demonstrates better performance than the MPPTs of similar category. However, the gain settings and tuning of PID controller are not properly discussed. An effective solution for detection of uniform and partial shading condition is proposed in [139]. This technique also partitions the regions based on integral multiples of V_{oc} of module. The algorithm complexity of this MPPT is high, nevertheless it outperforms several bio-inspired algorithms. Also, it performs well under fast varying weather conditions.

3.2.3. MPPTs incited from bio-inspired/physical phenomenon (Bio-I)

The techniques developed from the scientific philosophy of fuzzy logic, artificial neural network, neuro-fuzzy inference system etc., are comprehensively reviewed in [140–142]. Keeping in view the past literature survey and latest trend in the development of MPPTs, special emphasis is given to bio-inspired MPPTs in this section.

In the workspace of numerous local peaks, multiple variables/agents can be deployed to search the required target. Since these variables are operated in close association with each other, an optimization of multivariable function is essential [143]. Particle swarm optimization (PSO) is one of the renowned optimization method, which is inspired from the natural social behavior of biological species such as bird flocking and fish schooling [143]. Compared to other meta-heuristic optimization methods, PSO exhibits fast convergence speed and requires simple implementation. Therefore, it gains tremendous popularity in the searching of global maximum (GM), when PV array is under the influence of partial shading [143–146].

Consider an example of birds flocking: birds are the particles, which are living or working in a flock known as swarm, and their mutual cooperation enables them to reach the required target [143]. Since each particle in a swarm has its existence and thinking, it has some fitness value mapped by an objective function. Through its own fitness value and best fitness value of the swarm, each particle decides its future individual velocity, which will determine the new direction and position of the particle.

In accordance with the parameters of PV array, the PSO is transformed as follows: position (x_i) of each particle is modeled as operating voltage or duty cycle (*D*) of dc-dc converter [143,145], velocity (v_i) of each particle represents the step size and direction i.e., + /- ΔV or + /- Δ*D*, search space is I-V curve, and required target is the searching of GM. The working principle of PSO and its mapping with PV system is as follows:

	Physical phenomenon of PSO		**Mapping with PV system**
Step-1	In start, particles ($x_i(k)$) are randomly positioned on search plane to take the information. Where, *k* represents the present instant and *i* being the number of particles.	→	In the first iteration, operating voltage ($V_{pvi}(k)$) points or $D_i(k)$ values of converter are randomly selected to probe different operating points of I-V curve.
Step-2	Each particle has a fitness value mapped by an objective function, where P_{besti} is the personal best position and G_{besti} is the best position in the group or swarm.	→	The fitness value of each $V_{pvi}(k)$/$D_i(k)$ is determined through a power based objective function. The P_{besti} is the personal best operating point and G_{besti} is best operating point amongst all the $V_{pvi}(k)/D_i(k)$ values of I-V curve.
Step-3	Velocity ($v_i(k)$) of each particle is calculated on the basis of P_{besti} and G_{besti} as represented in Eq. (43)	→	The step size along with direction (+/- $\Delta V_i(k)$ or + /- $\Delta D_i(k)$) of each $D_{i(}k)$ is formulated through P_{besti} and G_{besti}.
Step-4	Future position ($x_i(k + 1)$) of particle is updated through velocity ($v_i(k)$) as represented in Eq. (44)	→	Future $V_{pvi}(k + 1)/(D_i(k + 1))$ of particle is updated through perturbation step + /- $V_{pvi}(k)$/ $\Delta D_i(k)$.

Goto Step-2

$$\underbrace{v_i(k+1)}_{New\ Velocity/\pm\Delta V_i(k+1)} = \underbrace{wv_i(k)}_{Velocity/\pm\Delta V_i(k)} + c_1 r_1\left(\underbrace{P_{besti}}_{LM_i} - \underbrace{x_i(k)}_{Position/Oper.pointV_{pvi}orD_i}\right) + c_2 r_2\left(\underbrace{G_{besti}}_{GM_i} - x_i(k)\right) \quad (43)$$

$$\underbrace{x_i(k+1)}_{New\ Position/New\ Oper.pointV_{pvi}orD_i} = \underbrace{x_i(k)}_{Position/Oper.pointV_{pvi}orD_i} + \underbrace{v_i(k+1)}_{New\ Velocity/\pm\Delta V_i(k+1)} \quad (44)$$

where, $i = 1,2,\ldots, N$ is number of particles, w is inertial weight, c_1 is cognitive coefficient, c_2 is social coefficient, r1 and r2 are random variables.

In start, a deterministic -PSO (DPSO) [145] randomly selects three D values of buck-boost converter. It then follows the aforementioned *Steps* with the exception that it removes the randomness of Eq. (43). It makes the solution deterministic and only w needs to be tuned. On similar terms, the random nature of PSO is removed in accelerated APSO [147]. This reduces the computation cost of MPPT and it can be implemented with low cost microcontroller. In [143], Lagrange Interpolation formula is used for better management of distributions of D. The Cuk converter is used by this MPPT. An overall distribution (OD) algorithm is merged with PSO in OD-PSO [148] to improve the tracking speed of PSO. In this method, a Cauchy distribution from the field of continuous probability distribution is applied for the better positioning of future particles *i.e.* D values.

It is pertinent to note that the majority of bio-inspired algorithms follow the same route as mentioned in above *Steps*. The main difference lies in the distinct objective functions involved in the estimation of velocity (step size and direction) and position. Generally, the objective functions are also based on power functions. In ant colony optimization (ACO), the homing strategy, in order to return to the nest, is executed through pheromone-based communication. Through this communication, the next ant movement and position is decided. A hybrid method is presented in ACO-PO [149], where the global and local search capability of algorithm is enhanced through ACO and PO respectively. For global search, the ant pollution is selected as 6 for I-V plane. The position of each ant is referred as D of the converter. The step size (δ) for an ant movement is calculated from Eq. (45) and the perturbation in D is calculated from Eq. (46).

$$\underbrace{\delta_i(k+1)}_{New\ Step/\pm\Delta V_i(k+1)} = \underbrace{\delta_0 e^{-k}}_{Step/\pm\Delta V_i(k+1)} \quad (45)$$

$$\underbrace{d_i(k+1)}_{New\ Position/New\ Oper.pointD_i} = \underbrace{d_i(k)}_{Position/Oper.pointD_i} + \underbrace{a \times \delta_i(k+1)}_{New\ Step/\pm\Delta V_i(k+1)} \quad (46)$$

where, a is the unit vector.

A gray wolf optimization method is adopted in GWO [150] for the detection of global maximum. In nature, gray wolves usually live in a pack and follow a leadership hierarchy for hunting of prey. For PV application, the D values of converter represent the wolves. The fitness value of each wolf is estimated through power based objective function. Finally, the new step size and future perturbation in D is calculated from Eq. (47) and Eq. (48), respectively. The whale optimization (WO) inspired from hunting behavior of humpback whale is merged with differential evolution (DE) in WODE [151]. The hunting behavior of whale involves searching, encircling and bubble-neck attacking on a prey, which is similar to hunting mechanism of GWO.

$$D = |Cx_i(k) - x_i(k)| \quad (47)$$

$$\underbrace{x_i(k+1)}_{Position\ vector\ of\ wolf/New\ Oper.pointD_i} = \underbrace{x_i(k)}_{Position\ vector\ of\ prey/Oper.pointD_i} - A \times D \quad (48)$$

where, A, C and D are coefficient vectors.

Fireflies are unisex and get attracted towards the brighter and attractive fireflies. The brightness of a firefly determines the fitness value, which depends upon the distance between itself and other flies. By using this information, the firefly movement and its new position is determined. A modified firefly algorithm is proposed in MFA [152], where the mapping of natural behavior of fireflies to PV system for the tracking of GM is accomplished as:

FA algorithm	→	**PV system**
Firefly position	→	Voltage reference (V_{ref})
Distance	→	Voltage step (ΔV_{ref})
Attractiveness	→	An exponential function of ΔV_{ref}
Brightness	→	Power (P_{best})
Brightness of the brightest firefly	→	Global maximum (G_{best})

Bats utilize the sonar based sensing to detect the prey and avoid obstacles. Likewise fireflies, which utilize the brightness to update their position and distance, bats use the frequency of sonar waves to calculate the future velocity and position as illustrated in Eq. (49) and Eq. (50) respectively. The MPPT based on foraging bat behavior is presented in BA [153], where chaos search strategy is introduced in bat algorithm for the better management of bats population.

$$\underbrace{v_i(k+1)}_{New\ Step/\pm\Delta V_i(k+1)} = \underbrace{v_i(k)}_{Step/\pm\Delta V_i(k)} + \underbrace{(xi(k) - x^*) \times Qi}_{Position/Oper.pointV_{pvi}} \quad (49)$$

$$\underbrace{x_i(k+1)}_{New\ Position/New\ Oper.pointV_{pvi}} = \underbrace{x_i(k)}_{Position/Oper.pointV_{pvi}} + \underbrace{v_i(k)}_{Step/\pm\Delta V_i(k)} \quad (50)$$

where, x^* is the best position, and Q_i is the varying frequency.

In artificial bee colony (ABC) algorithm [154], the vector solution revolves around the position and food amount of a nectar source. Three groups of bees are working for it: 1) employee bees, onlooker bees, and 3) scout bees. The employee bees always update the more enriched nectar source through visual information and discard the location of previous source, while onlooker bees move towards the new nectar source discovered by employee bees. The mapping of ABC with PV system is implemented in ABC [154] by replacing the nectar amount with PV power and variations in food source position with the perturbation in D. Likewise previous algorithms, random values of D of converter initiate the initial positions of bees. In cat swam optimization (CAT) [155], all cats search for an optimal position through two different searching modes, primarily known as seeking mode and tracking mode. Each cat in a group contains its individual velocity and position. The algorithm is similar to PSO, where position of each particle represents the D value of converter. Through its own position Eq. (51) and the best position amongst the swarm, a new velocity of each cat is determined through Eq. (52).

$$\underbrace{v_i(k+1)}_{New\ Velocity/\pm\Delta V_i(k+1)} = \underbrace{wv_i(k)}_{Velocity/\pm\Delta V_i(k)} + c_1 r_1\left(\underbrace{x_{besti}}_{Best\ Position} - \underbrace{x_i(k)}_{Position/Oper.pointV_{pvi}orD_i}\right) \quad (51)$$

$$\underbrace{x_i(k+1)}_{New\ Position/New\ Oper.pointV_{pvi}orD_i} = \underbrace{x_i(k)}_{Position/Oper.pointV_{pvi}orD_i} + \underbrace{v_i(k+1)}_{New\ Velocity/\pm\Delta V_i(k+1)} \quad (52)$$

where, $i = 1,2,\ldots, N$ is number of cats, w is inertial weight, c_1 is acceleration constant, r1 is a random number ranging from 0 to 1.

The MPPT algorithm based on flower pollination is presented in [156], where the natural phenomenon of self-pollination and cross-pollination of flowers are mapped for the local maximum and global maximum of PV system. A monkey king evolution algorithm inspired from mythological novel is presented in MK [157]. In the eve of unfavorable scenario, the monkey king has the power to convert himself into several monkeys. Each monkey finds out the solution and reports to the monkey king. After receiving the information, the monkey king

Table 3
Mapping of natural environment of Bio-I mechanism to PV system.

Bio-Inspired MPPTs	Particles - *Serves as operating points (V_{pv} or D)*	Nature working plane - *Transformed into I-V plane*	Required target - *Mimcks the global maximum (GM) on P-V curve*	Particles initialization – *Particles thrown for initial probing of I-V curve*	Involvement of fitness function for each particle – *To identify the GM amongst the particles*	Mathematical functions plus coefficients for position and voltage steps – *To estimate new operating points on P-V curve with perturbation steps*
PSO [143] OD-PSO [148]	Birds	Traveling in a group for migration	Best position or trajectory amongst the birds	Random	Yes	Random variables r1 and r2 Coefficients: w interial weight
ACO [149]	Ants	Homing strategy to return home through pheromone-based communication	Best position amongst the ants	Fixed	Yes	Exponential and unit vector
GWO [150]	Gray wovles	Hunting mechanism of gray wolves	Best position to catch prey	Random	Yes	Cosine and random functions, vector coefficients A,D, C
WODE [151]	Humpback whales	Hunting mechanism of humpback whale	Best position to catch prey	Random	Yes	Random fucntions and coefficients, Cosine function and vector coefficient A, Cross-over and mutation factor
MFA [152]	Fireflies	Most attractive fireflies amongst the groups	Fireflies with best brightness	Random	Yes	Random perturbation value, initial attractiveness β_o, absorption coefficient γ
BA [153]	Bats	Hunting of prey and obstacle avoidance	Best position calculated through sonar waves (frequency)	Random	Yes	Random fucntion, loundness wave coefficient α, pulse rate coefficient γ
ABC [154]	Employee and onlooker bees	Identification of nectar source with best food amount	Best nectar source through visual inspection	Random	Yes	Random fucntion ϕ, adaptation weight A_w
CAT [155]	Cats	Searching of safe location	Best position amongst the group	Random	Yes	Random fucntions and coefficients, acceleration coefficient c_1, intertial weight w_1, and standard deviation
Flower [156]	Flowers	Pollination process of flower through pollen transfers from species	Best reproduction constancy of flower	Random	Yes	Switching pollen probability P, pollen transfer levy factor L, local search in distribution $\mathcal{E}$
MK [157]	Monkeys (Monkey king transformed into several monkeys)	Optimal solution in difficult situation	Best solution received from the monkeys	Random	Yes	Random fucntion, fluctuation coefficient F_c, random transformation matrix size, binary reversal factor, mutation operator a
MFO [158]	Moths	Traversing towards light source such as moon light or artificial light in night	Best flames (light source)	Random	Yes	Exponential and cosine functions, coefficients factor
Fire [159]	Fireworks	Explosion of fireworks in the sky	Optimal explosion of fireworks	Random	Yes	Random numbers and fucntions, fireworks coefficients
DE [160]	Vectors	Global searching	Optimal point	Fixed	Yes	Mutation factor F, randon number with cross over rate CR
SA [161]	Temperature values	Anealing process in metals	Minimum energy to cool matters	Random	No	Acceptance probability P_r and exponential functions.

Table 4
Comparison table and overall rating of MPPTs.

MPPT	Classification	Algorithm's Complexity (1–5) in accordance with Section 2.1	Hardware Implementation (1–5) in accordance with Section 2.2	Tracking Speed (1–3) in accordance with Section 2.3	Accuracy of GM detection (1–3) in accordance with Section 2.5	Overall Rating according to Eq. (2)	Search/ Control Variable	Converter	Load Application
MPPT [126]	I-V tracer	1	4	1	1	1.5	Duty	Boost	Resistive
MPPT [127]	I-V tracer (Series Capacitor)	1	4	1	1	1.5	Voltage	Boost	Battery
MPPT [129]	Voltage Zone (Bypass diode based)	3	4	2	1	2.16	Voltage	Boost	Resistive
MPPT [132]	Voltage Zone (String based)	3	3	2	1	2	Voltage	Boost	Resistive
MPPT [133]	Voltage Zone (Restricted voltage window based)	3	3	2	1	2	Voltage	Inverter	Grid
MPPT [134]	Voltage Zone (Reduced voltage range)	3	3	2	1	2	Voltage	Inverter	Grid
MPPT [135]	Voltage Zone	3	2	2	1	1.83	Voltage	Boost	Battery
MPPT [136]	Voltage Zone	3	3	2	1	2	Voltage	Boost	Resistive
MPPT [137]	Voltage Zone (Partition estimation based)	3	3	2	2	2.33	Voltage	Buck	Battery
MPPT [138]	Voltage Zone (Approximating I-V curve based)	3	3	2	1	2	Voltage	Boost	Battery
MPPT [139]	Voltage Zone	3	3	2	1	2	Voltage	Buck-Boost	Resistive
PSO [143]	Bio-Inspired (Particle swarm)	4	1	3	1	2.16	Duty	Cuk	Resistive
OD-PSO [148]	Bio-Inspired (Overall Distribution - Particle swarm)	5	1	3	1	2.33	Duty	Buck	Resistive
ACO [149]	Bio-Inspired (Ant colony)	4	1	3	1	2.16	Duty	Boost	Resistive
GWO [150]	Bio-Inspired (Gray wolf)	4	1	3	1	2.16	Duty	Boost	Resistive
WODE [151]	Bio-Inspired (Whale optimization)	5	1	3	1	2.33	Duty	Boost	Battery
MFA [152]	Bio-Inspired (Fire-Fly algorithm)	5	1	3	1	2.33	Voltage	Interleaved Boost	Resistive
BA [153]	Bio-Inspired (Bat algorithm)	5	1	3	1	2.33	Voltage	Boost	Resistive
ABC [154]	Bio-Inspired (Artificial bee colony)	4	1	3	1	2.16	Duty	Boost	Resistive
CAT [155]	Bio-Inspired (Cat algorithm)	4	1	3	1	2.16	Duty	Boost	Resistive (Electronic load)
Flower [156]	Bio-Inspired (Flower pollination)	5	1	3	1	2.33	Duty	Boost	Resistive
MK [157]	Bio-Inspired (Monkey king algorithm)	5	1	3	1	2.33	Duty	Boost	Battery
MFO [158]	Bio-Inspired (Moth algorithm)	5	1	3	1	2.33	Duty	Boost	Grid
Fire [159]	Physical phenomenon (Fireworks optimization)	5	1	3	1	2.33	Duty	Boost	Resistive
DE [160]	Bio-Inspired (Differential evolution)	4	1	3	1	2.16	Duty	SEPIC	Resistive
SA [161]	Physical phenomenon (Cooling of metals)	3	1	3	2	2.33	Voltage	Boost	–

filters the most feasible solution and then directs the monkeys to move towards the target accordingly. In PV system, the monkey king creates several D values of converter, and after receiving the power from each D value, it finds out the global power. Thereafter, it updates the global best solution from Eq. (53) and updates the D values with the solution proposed in Eq. (54).

$$\underbrace{d_{gbest}(k+1)}_{\text{Update Best Solution/New Oper.pointD}} = \underbrace{d_{gbest}(k)}_{\text{Prev Best Solution/Prev Oper.pointD}} + F_c \times d_{diff} \tag{53}$$

$$\underbrace{d(k+1)}_{\text{Update Others Solution/New Oper.pointD}} = \underbrace{Mi \otimes d(k)}_{\text{Prev Others Solution/Prev Oper.pointD}} + B \tag{54}$$

where, F_c is fluctuation coefficient, *diff* is the random difference between two random variables, M_i is the binary reversal at iteration i, $\otimes$ denotes the element multiplication.

From the field of meta-heuristic optimization, a moth-flame optimization (MFO) algorithm is proposed in MFO [158] to solve the problem of GM tracking. The algorithm works on the flying principle of moth, which maintains a constant angle with respect to the nearest light source. This optimization revolves around the movement of moths (n) and flames populations in the research space (d). Both moths and flames are vector quantities, the positions of these play a vital role in detecting the GM. The positions of moths and flames are transformed into operating V_{pv} points and P_{pv} points respectively in the research space of I-V curve. A four-step layout is proposed in MFO [158], which is as follows: 1) the random distribution function is used to initialize the moths positions, 2) the research space of moths is checked and moths fitness is computed, 3) the best positions and values of flames is updated, and 4) finally, the moths position is updated with regard to flames position. The MFO [158] based controller directly controls the duty cycle of dc-dc converter to optimize the operation of incremental conductance (IC) method.

In [159], a global minimization algorithm based on explosion of fireworks in the sky is proposed for the detection of GM in PV array. An improved differential evolution is presented in [160], where the GM of PV array is tracked through SPEIC converter and load variations. Annealing process used in metallurgy is essentially a random search process guided by temperature parameters that can accept a worst operating point under certain conditions. Simulated annealing based MPPT algorithm explores the search space and leads to global peak for both uniform and non-uniform conditions SA [161]. An MPPT based on Cuckoo search is presented in [162] to track the global peak of medium as well as large PV systems. This MPPT achieves better performance than both P&O and PSO algorithms under shading conditions.

Table 3 encapsulates the mapping of natural/physical environment and behavior of biological organisms with the PV system. In table, second column indicates the particles behaving as D or V_{pv} values in PV system. Similarly, the third and fourth columns show the mapping of natural working plane with I-V plane and required target with global maximum (GM), respectively. The last column depicts the complex mathematical operations required to compute the future operating points and perturbation steps.

In these methods, the following considerations and improvements are put forward for the new designers:

- In majority of the methods, population of particles and their spread on I-V search plane is random. Since size of I-V plane and number of particles may vary with different array sizes, a proper study is needed, which should clearly define the population of particles with regard to array size.
- The bio-inspired MPPTs have compatibility and scalability issues i.e. all the parameters need to be reconfigured or retuned with different array sizes.
- The spread of particles (duty cycle values of converter) with distinct loads is not comprehensively discussed.
- Bio-inspired methods are complex in nature as they require random distribution functions and complex mathematical operations. A high-tech embedded system with fast sampling rate of A/D converters is required to install these MPPTs in PV system.
- There are number of coefficients and other key parameters involved in the mathematical operation. The tuning of these parameters is not usually formulated and instead a constant value is awarded.
- The involvement of numerous iterations, where in each iteration new position (operating point) and velocity (± voltage step) are computed, makes the computation burden and cost of Bio-I algorithms high.
- Most methods use V_{oc} or I_{sc} values in their operations, however robust estimation of these key parameters is a missing link in Bio-I MPPTs.
- Generally, these methods start their operation with an assumption that new condition is a partial shading condition. Thus, these methods cannot conveniently differentiate between uniform and partial shading conditions.

3.2.4. Comparison table of partial shading MPPTs

The three different types of MPPTs for partial shading conditions are summarized in Table 4, where the overall rating of each MPPT is estimated through formulations proposed in Section 2. It can be deduced from table that I-V curve tracing MPPTs exhibit the highest tracking speed, nevertheless they require additional hardware arrangement in the PV system. The MPPTs derived from the power-voltage characteristics of PV array also show good efficiency. Since numerous iterations along with several particles are involved in Bio-Inspired algorithms, they exhibit less tracking speed compared to others. However, in terms of hardware requirements, they are better than I-V curve tracer MPPTs. In the end, a unique graph is presented in Fig. 16, which indicates the progression tree of the development of MPPTs with years. This graph also outlines the comparison between different MPPTs and provides awareness to new MPPT researchers in the selection of benchmark method.

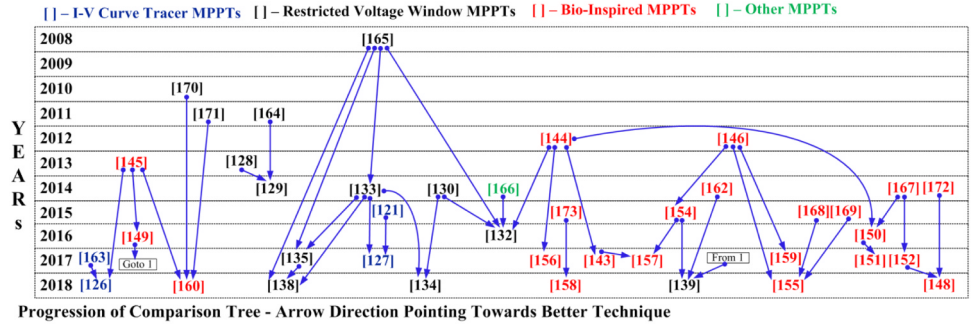

Fig. 16. Progression tree between MPPTs with years [163-173].

4. Conclusion

The cost effective and efficient extraction of maximum power from PV array depends on the MPPT control strategy. This paper presents review of various MPPT techniques, which are explained with block and schematic diagrams, working principles, algorithms, and their pros and cons. This review explores the input, output and hidden parameters of MPPT techniques under uniform, rapidly changing and partial shading conditions. This paper concludes that most of the conventional MPPT algorithms operate PV array at MPP under uniform weather conditions and fail to obtain true MPP under rapidly changing and partial shading conditions. The intelligent and advanced algorithms drive PV array at true MPP under partial shading and rapidly changing conditions, however, they are complex algorithms and, therefore, difficult to implement using embedded technologies. This paper also provides evaluation criteria for various MPPT algorithms which can help the MPPT developers to pick a convenient technique for any desired PV system. The potential application areas of the reviewed papers have also been addressed in the form of Tables, where the load (resistive, inductive, battery and grid) of MPPTs are mentioned. Following are some noteworthy recommendations:

- Classical hill climbing methods are the most widely used algorithms in commercial applications, however; they suffer from continuous power oscillations around MPP and have the tendency to operate in wrong direction under rapidly changing atmospheric conditions. Nevertheless, researchers have developed intelligent controlling techniques to operate PV array at optimal point under all weather conditions.
- Fractional MPPT methods are approximate methods to obtain MPP. However, they are fast and the least expensive.
- Under partial shading case, curve tracing MPPTs show best convergence speed with high efficiency in detecting the global maximum. However, their practical implementation requires additional hardware. MPPTs based on voltage restricted window have mediocre complexity and efficiency. Bio inspired MPPT algorithms are also accurate methods under partial shading conditions. They are however, not easy to implement because of the innate high complexity of algorithms. Obviously, sophisticated embedded system is required for the implementation of these MPPTs. In addition, high level programming skills are required to translate the algorithm for embedded controller.
- A complete ranking criterion is introduced and formulated, which can be applied on any MPPT to rank its effectiveness.
- The tree network shown in Fig. 16 provides a historical perspective of the development of partial shading algorithm that will act as a beacon for the future researchers in understanding the evolution of MPPT methods.

References

[1] Pandey A, Tyagi V, Jeyraj A, Selvaraj L, Rahim N, Tyagi S. Recent advances in solar photovoltaic systems for emerging trends and advanced applications. Renew Sustain Energy Rev 2016;53(0):859–84.
[2] Erdinc O, Uzunoglu M. Optimum design of hybrid renewable energy systems: overview of different approaches. Renew Sustain Energy Rev 2012;16(3):1412–25.
[3] Hosseinzadeh HB, Tabatabaei M, Aghbashlo M, Khanali M, Demirbas A. A comprehensive review on the environmental impacts of diesel/biodiesel additives. Energy Convers Manag 2018;174(0):579–614.
[4] Whiting K, Carmona LG, Sousa T. A review of the use of energy to evaluate the sustainability of fossil fuels and non-fuel mineral depletion. Renew Sustain Energy Rev 2017;76(0):202–11.
[5] F. B. Mid-term renewable energy market report; 2015.
[6] Aanesen K, Heck S, Pinner D. Solar power. Darkest before dawn; 2017.
[7] Jazayeri M, Jazayeri K, Uysal S. Adaptive photovoltaic array reconfiguration based on real cloud patterns to mitigate effects of non-uniform spatial irradiance profiles. Sol Energy 2017;155(0):506–16.
[8] Bouselham L, Hajji B, Mellit A, Rabhi A, Mazari A. A reconfigurable pv architecture based on new irradiance equalization algorithm. In: Proceedings of international conference on electronic engineering and renewable energy; 2018. p. 470–7.
[9] Belhaouas N, Cheikh MSA, Agathoklis A, Oularbi MR, Amrouche B, Sedraoui K, Djilali N. PV array power output maximization under partial shading using new shifted pv array arrangements. Appl Energy 2017;187(0):326–37.
[10] Merino S, Sa´nchez F, Cardona MSD, Guzman F, Guzman R, Martınez J, Sotorrıo P. Optimization of energy distribution in solar panel array configurations by graphs and minkowski's paths. Appl Math Comput 2018;319(0):48–58.
[11] Khan O, Xiao W. An efficient modeling technique to simulate and control sub-module-integrated pv system for single-phase grid connection. IEEE Trans Sustain Energy 2016;7(1):96–107.
[12] Adly M, Strunz K. Irradiance-adaptive pv module integrated converter for high efficiency and power quality in standalone and dc microgrid applications. IEEE Trans Ind Electron 2018;65(1):436–46.
[13] Pan CT, Cheng MC, Lai CM, Chen PY. Current-ripple-free module integrated converter with more precise maximum power tracking control for pv energy harvesting. IEEE Trans Ind Appl 2015;51(1):271–8.
[14] Sher HA, Murtaza AF, Al-Haddad K. A hybrid maximum power point tracking method for photovoltaic applications with reduced offline measurements. In: Proceedings of IEEE international conference on industrial technology (ICIT); 2017. p. 1482–5.
[15] Ghasemi MA, Foroushani HM, Parniani M. Partial shading detection and smooth maximum power point tracking of pv arrays under psc. IEEE Trans Power Electron 2016;31(9):6281–92.
[16] Tafti HD, Maswood HI, Konstantinou G, Pou J, Blaabjerg F. A general constant power generation algorithm for photovoltaic systems. IEEE Trans Power Electron 2018;33(5):4088–101.
[17] Benyoucef AS, Chouder A, Kara K, Silvestre S. Artificial bee colony based algorithm for maximum power point tracking (mppt) for pv systems operating under partial shaded conditions. Appl Soft Comput 2015;32:38–48.
[18] Oshaba A, Ali E, Elazim SA. Mppt control design of pv system supplied srm using bat search algorithm. Sustain Energy Grids Netw 2015;2(0):51–60.
[19] Ahmad R, Murtaza AF, Sher HA, Shami UT, Olalekan S. An analytical approach to study partial shading effects on PV array supported by literature. Renew Sustain Energy Rev 2017;76(0):407–24.
[20] Noguchi T, Togashi S, Nakamoto R. Short-current pulse-based maximum-power-point tracking method for multiple photovoltaic-and-converter module system. IEEE Trans Ind Electron 2002;49(1):217–23.
[21] Sher HA, Murtaza AF, Addoweesh KE, Al-Haddad K, Chiaberge M. A new irradiance sensorless hybrid mppt technique for photovoltaic power plants. In: Proceedings of the 40th annual conference of the IEEE industrial electronics society, IECON; 2014. p. 1919–23.
[22] Masoum MA, Dehbonei H, Fuchs EF. Theoretical and experimental analyses of photovoltaic systems with voltage and current-based maximum power-point tracking. IEEE Trans Energy Convers 2002;17(4):514–22.
[23] Faranda R, Leva S. Energy comparison of mppt techniques for pv systems. WSEAS Trans Power Syst 2008;3(6):446–55.
[24] Sher HA, Murtaza AF, Noman A, Addoweesh KE, Chiaberge M. An intelligent control strategy of fractional short circuit current maximum power point tracking technique for photovoltaic applications. J Renew Sustain Energy 2015;7(1):113–4.
[25] Hsu TW, Wu HH, Tsai DL, Wei CL. Photovoltaic energy harvester with fractional open-circuit voltage based maximum power point tracking circuit. IEEE Trans Circ Syst II: Express Briefs 2018.
[26] Murtaza A, Sher H, Chiaberge M, Boero D, Giuseppe MD, Addoweesh K. Comparative analysis of maximum power point tracking techniques for pv applications. In: Proceedings of multi topic conference (INMIC); 2013. p. 83–8.
[27] Tariq A, Asghar J. Development of an analog maximum power point tracker for photovoltaic panel. In: Proceedings of IEEE international conference on power electronics and drives systems. Vol. 1; 2005. p. 251–5.
[28] Liu F, Kang Y, Zhang Y, Duan S. Comparison of p & o and hill climbing mppt methods for grid-connected pv converter. In: Proceedings of 3rd IEEE conference on IEEE industrial electronics and applications. ICIEA;, 2008. p. 804–7.
[29] Xiao W, Dunford WG. A modified adaptive hill climbing mppt method for photovoltaic power systems. In: Proceedings of IEEE 35th annual power electronics specialists conference. PESC 04. Vol. 3; 2004. p. 1957–63.
[30] Elgendy MA, Zahawi B, Atkinson DJ. Assessment of perturb and observe mppt algorithm implementation techniques for pv pumping applications. IEEE Trans Sustain Energy 2012;3(1):21–33.
[31] Jordehi AR. Maximum power point tracking in photovoltaic (pv) systems: a review of different approaches. Renew Sustain Energy Rev 2016;65:1127–38.
[32] Kamarzaman NA, Tan CW. A comprehensive review of maximum power point tracking algorithms for photovoltaic systems. Renew Sustain Energy Rev 2014;37:585–98.
[33] Gupta A, Chauhan YK, Pachauri RK. A comparative investigation of maximum power point tracking methods for solar pv system. Sol Energy 2016;136:236–53.
[34] Kwan TH, Wu X. An adaptive scale factor based mppt algorithm for changing solar irradiation levels in outer space. Acta Astronaut 2017;132:33–42.
[35] Yang Y, Zhao FP. Adaptive perturb and observe mppt technique for grid-connected photovoltaic inverters. Procedia Eng 2011;23:468–73.
[36] Tan CW, Green TC, Hernandez CAA. An improved maximum power point tracking algorithm with current-mode control for photovoltaic applications. In: Proceedings of IEEE conference on power electronics and drives systems. Vol. 1; 2005. p. 489–94.
[37] Femia N, Petrone G, Spagnuolo G, Vitelli M. Power electronics and control techniques for maximum energy harvesting in photovoltaic systems. CRC Press; 2012.
[38] Jung Y, So J, Yu G, Choi J. Improved perturbation and observation method (i p & o) of mppt control for photovoltaic power systems. In: Conference record of the Thirty-first IEEE photovoltaic specialists conference. IEEE; 2005. p. 1788–91.

[39] Yin T, Meng X, Wang Z, Lin C. Maximum power point tracking based on adaptive p &o method. In: Proceedings of IEEE workshop on electronics, computer and applications; 2014. p. 261–4.
[40] Ji YH, Jung DY, Won CY, Lee BK, Kim JW. Maximum power point tracking method for pv array under partially shaded condition. In: Proceedings of energy conversion congress and exposition IEEE; 2009. p. 307–12.
[41] Mei Q, Shan M, Liu L, Guerrero JM. A novel improved variable step-size incremental-resistance mppt method for pv systems. IEEE Trans Ind Electron 2011;58(6):2427–34.
[42] Tan CY, Rahim NA, Selvaraj J. Employing dual scaling mode for adaptive hill climbing method on buck converter. IET Renew Power Gener 2015.
[43] Kasa N, Lida T, Iwamoto H. Maximum power point tracking with capacitor identifier for photovoltaic power system. In: Proceedings of IEE electric power applications. Vol. 147, no. 6; 2000. p. 497–502.
[44] Podgurski RCP, Perreault DJ. Submodule integrated distributed maximum power point tracking for solar photovoltaic applications. IEEE Trans Power Electron 2013;28(6):2957–67.
[45] Hua CC, Fang YH, Wong CJ. Improved solar system with maximum power point tracking. IET Renew Power Gener 2018;12(7):806–14.
[46] Liu F, Duan S, Liu F, Liu B, Kang Y. A variable step size inc mppt method for pv systems. IEEE Trans Ind Electron 2008;55(7):2622–8.
[47] Liu B, Duan S, Liu F, Xu P. Analysis and improvement of maximum power point tracking algorithm based on incremental conductance method for photovoltaic array. In: Proceedings of IEEE international conference on power electronics and drive systems; 2007. p. 637–41.
[48] Zhao J, Zhou X, Gao Z, Ma Y, Qin Z. A novel global maximum power point tracking strategy (gmppt) based on optimal current control for photovoltaic systems adaptive to variable environmental and partial shading conditions. Sol Energy 2017;144:767–79.
[49] Tousi S, Moradi M, Basir NS, Nemati M. A function based maximum power point tracking method for photovoltaic systems. IEEE Trans Power Electron 2015;99. [0] [: 1–1].
[50] Kadri R, Gaubert JP, Champenois G. An improved maximum power point tracking for photovoltaic grid-connected inverter based on voltage- oriented control. IEEE Trans Ind Electron 2011;58(1):66–75.
[51] Mutoh N, Ohno M, Inoue T. A method for mppt control while searching for parameters corresponding to weather conditions for pv generation systems. IEEE Trans Ind Electron 2006;53(4):1055–65.
[52] Urayai C, Amaratunga GA. Single-sensor maximum power point tracking algorithms. Renew Power Gener IET 2013;7(1):82–8.
[53] Kasa N, Iida T, Chen L. Flyback inverter controlled by sensorless current mppt for photovoltaic power system. IEEE Trans Ind Electron 2005;52(4):1145–52.
[54] Moon S, Kim SJ, Seo JW, Park JH, Park C, Chung CS. Maximum power point tracking without current sensor for photovoltaic module integrated converter using zigbee wireless network. Int J Electr Power Energy Syst 2014;56(0):286–97.
[55] Ryu DK, Choi BY, Lee SR, Kim YH, Won CY. Flyback inverter using voltage sensorless mppt for photovoltaic ac modules. J Power Electron 2014;14(6):1293–302.
[56] Shmilovitz D. On the control of photovoltaic maximum power point tracker via output parameters. In: IEE proceedings of electric power applications. IET. vol. 152; no. 2; 2005. p. 239–48.
[57] Jiang Y, Qahouq JAA, Haskew T. Adaptive step size with adaptive-perturbation-frequency digital mppt controller for a single-sensor photovoltaic solar system. IEEE Trans Power Electron 2013;28(7):3195–205.
[58] Shimizu T, Hashimoto O, Kimura G. A novel high-performance utility-interactive photovoltaic inverter system. IEEE Trans Power Electron 2003;18(2):704–11.
[59] Gao M, Chen M, Zhang C, Qian Z. Analysis and implementation of an improved flyback inverter for photovoltaic ac module applications. IEEE Trans Power Electron 2014;29(7):3428–44.
[60] Petrone G, Spagnuolo G, Vitelli M. A multivariable perturb-and-observe maximum power point tracking technique applied to a single-stage photovoltaic inverter. IEEE Trans Ind Electron 2011;58(1):76–84.
[61] Jiang J, Huang T, Hsiao Y, Chen C. Maximum power tracking for photovoltaic power systems. Tamkang J Sci Eng 2005;8(2):147.
[62] Sera D, Kerekes T, Teodorescu R, Blaabjerg F. Improved mppt algorithms for rapidly changing environmental conditions. In: Proceedings of IEEE power electronics and motion control conference; 2006. p. 1614–9.
[63] Alonso R, Ibaez P, Martinez V, Roman E, Sanz A. An innovative perturb, observe and check algorithm for partially shaded pv systems. In: Proceedings of IEEE European conference on power electronics and applications; 2009. p. 1–8.
[64] Yu B. An improved dynamic maximum power point tracking method for pv application. IEICE Electron Express 2014;11(2). [20 130 941– 20 130 941].
[65] Furtado AM, Bradaschia F, Cavalcanti MC, Limongi LR. A reduced voltage range global maximum power point tracking algorithm for photovoltaic systems under partial shading conditions. IEEE Trans Ind Electron 2018;65(4):3252–62.
[66] Kumar N, Hussain I, Singh B, Panigrahi BK. Framework of maximum power extraction from solar pv panel using self predictive perturb and observe algorithm. IEEE Trans Sustain Energy 2018;9(2):895–903.
[67] Kumar N, Hussain I, Singh B. Self-adaptive incremental conductance algorithm for swift and ripple-free maximum power harvesting from pv array. IEEE Trans Ind Inform 2018;14(5):2031–41.
[68] Reisi AR, Moradi MH, Jamasb S. Classification and comparison of maximum power point tracking techniques for photovoltaic system: a review. Renew Sustain Energy Rev 2013;19(0):433–43.
[69] Tey KS, Mekhilef S. Modified incremental conductance algorithm for photovoltaic system under partial shading conditions and load variation. IEEE Trans Ind Electron 2014;61(10):5384–92.
[70] Tey KS, Mekhilef S. Modified incremental conductance mppt algorithm to mitigate inaccurate responses under fast-changing solar irradiation level. Sol Energy 2014;101(0):333–42.
[71] Faraji R, Rouholamini A, Naji HR, Fadaeinedjad R, Chavoshian MR. Fpga-based real time incremental conductance maximum power point tracking controller for photovoltaic systems. IET Power Electron 2014;7(5):1294–304.
[72] Putri RI, Wibowo S, Rifai M. Maximum power point tracking for photovoltaic using incremental conductance method. Energy Procedia 2015;68(0):22–30.
[73] Hsieh GC, Hsieh HI, Tsai CY, Wang CH. Photovoltaic power-increment-aided incremental-conductance mppt with two-phased tracking. IEEE Trans Power Electron 2013;28(6):2895–911.
[74] Srinivas CL, Sreeraj E. A maximum power point tracking technique based on ripple correlation control for single-phase photovoltaic system with fuzzy logic controller. Energy Procedia 2016;90(0):69–77.
[75] Kimball JW, Krein PT. Discrete-time ripple correlation control for maximum power point tracking. IEEE Trans Power Electron 2008;23(5):2353–62.
[76] Casadei D, Grandi G, Rossi C. Single-phase single-stage photovoltaic generation system based on a ripple correlation control maximum power point tracking. IEEE Trans Energy Convers 2006;21(2):562–8.
[77] Subudhi B, Pradhan R. A comparative study on maximum power point tracking techniques for photovoltaic power systems. IEEE Trans Sustain Energy 2013;4(1):89–98.
[78] Tse K, Ho M, Chung HM, Hui S. A novel maximum power point tracker for pv panels using switching frequency modulation. IEEE Trans Power Electron 2002;17(6):980–9.
[79] Santos OL, Garcia G, Martinez SL, Giral R, Vidal EI, Merchan MCR, Yamel MG. Analysis, design and implementation of a static conductance-based mppt method. IEEE Trans Power Electron 2018.
[80] Khatib TT, Mohamed A, Amin N, Sopian K. An efficient maximum power point tracking controller for photovoltaic systems using new boost converter design and improved control algorithm. WSEAS Trans Power Syst 2010;5(2):53–63.
[81] Farayola AM, Hasan AN, Ali A. Curve fitting polynomial technique compared to anfis technique for maximum power point tracking. In: Proceedings of IEEE renewable energy congress (IREC); 2017. p. 1–6.
[82] Batzelis EI, Kampitsis GE, Papathanassiou SA. Power reserves control for pv systems with real-time mpp estimation via curve fitting. IEEE Trans Sustain Energy 2017;8(3):1269–80.
[83] Tay S, Lim I, Ye Z, Yang D, Garrigos A. Pv parameter identification using reduced iv data. In: Proceedings of IECON 2017-43rd annual conference of the IEEE industrial electronics society. IEEE; 2017. p. 2653–7.
[84] Yu WL, Lee TP, Wu GH, Chen QS, Chiu HJ, Lo YK, Shih F. A dsp-based single-stage maximum power point tracking pv inverter. In: Proeedings of twenty-fifth annual IEEE applied power electronics conference and exposition (APEC). IEEE; 2010. p. 948–52.
[85] Anoop K, Nandakumar M. A novel maximum power point tracking method based on particle swarm optimization combined with one cycle control. In: Proceedings of 2018 international conference on power, instrumentation, control and computing (PICC). IEEE; 2018. p. 1–6.
[86] Neto JTDC, Salazar AO, Costa AHD, Leite AC. One-cycle control based maximum power point tracker using constant voltage method for battery charging applications. In: Proceedings of IEEE power electronics conference (COBEP). Brazilian; 2017. p. 1–7.
[87] Salas V, Olias E, Barrado A, Lazaro A. Review of the maximum power point tracking algorithms for stand-alone photovoltaic systems. Sol Energy Mater Sol Cells 2006;90(11):1555–78.
[88] Carvalho PD, Pontes R, Oliveira D, Riffel D, Oliveira RD, Mesquita S. Control method of a photovoltaic powered reverse osmosis plant without batteries based on maximum power point tracking, In: Proceedings of transmission and distribution conference and exposition: Latin America. 2004 IEEE/PES. IEEE; 2004. p. 137–42.
[89] Sarkar PR. Maximum power point tracking method based on constant voltage for solar pv system. J Electr Power Syst Eng 2017;3(2).
[90] Park M, Yu IK. A study on the optimal voltage for mppt obtained by surface temperature of solar cell. In: Proceedings of 30th annual conference of IEEE industrial electronics society. IECON. vol. 3; 2004. p. 2040–5.
[91] Brito MAGD, Galotto L, Sampaio LP, GDEA Melo, Canesin CA. Evaluation of the main mppt techniques for photovoltaic applications. IEEE Trans Ind Electron 2013;60(3):1156–67.
[92] Solodovnik EV, Liu S, Dougal RA. Power controller design for maximum power tracking in solar installations. IEEE Trans Power Electron 2014;19(5):1295–304.
[93] Li X, Li Y, Seem JE, Lei P. Maximum power point tracking for photovoltaic systems using adaptive extremum seeking control. In: Proceedings of ASME 2011 dynamic systems and control conference and bath/ASME symposium on fluid power and motion control. American Society of Mechanical Engineers; 2011. p. 803–10.
[94] Bizon N. Searching of the extreme points on photovoltaic patterns using a new asymptotic perturbed extremum seeking control scheme. Energy Convers Manag 2017;144(0):286–302.
[95] Petrone G, Spagnuolo G, Vitelli M. An analog technique for distributed mppt pv applications. IEEE Trans Ind Electron 2012;59(12):4713–22.
[96] Petrone G, Spagnuolo G, Vitelli M. Teodi: a new technique for distributed maximum power point tracking pv applications. In: Proceedings of IEEE international conference on industrial technology (ICIT); 2010. p. 982–7.
[97] Balato M, Costanzo L, Marino P, Rubino G, Rubino L, Vitelli M. Modified teodi mppt technique: theoretical analysis and experimental validation in uniform and mismatching conditions. IEEE J Photovolt 2017;7(2):604–13.
[98] Petrone G, Spagnuolo G, Vitelli M. Teodi: Pv mppt based on the equalization of the

output operating points in correspondence of the forced displacement of the input operating points. In: Proceedings of IEEE international symposium on industrial electronics; 2010. p. 3463–8.
[99] Zhang L, Hurley WG, Wolfle W. A new approach to achieve maximum power point tracking for pv system with a variable inductor. In: Proceedings of power electronics for distributed generation systems (PEDG); 2010. p. 948–52.
[100] Wang P, Zhu H, Shen W, Choo FH, Loh PC, Tan KK. A novel approach of maximizing energy harvesting in photovoltaic systems based on bisection search theorem. In: Proceedings of twenty-fifth annual IEEE applied power electronics conference and exposition (APEC). IEEE; 2010. p. 2143–8.
[101] Yuvarajan S, Shoeb J. A fast and accurate maximum power point tracker for pv systems. In: Proceedings of applied power electronics conference and exposition; 2008. p. 167–72.
[102] Raj CM, Jeyakumar AE. A two stage successive estimation based maximum power point tracking technique for photovoltaic modules. Sol Energy 2014;103(0):43–61.
[103] Tafticht T, Agbossou K, Doumbia M, Cheriti A. An improved maximum power point tracking method for photovoltaic systems. Renew Energy 2008;33(7):1508–16.
[104] Moradi MH, Reisi AR. A hybrid maximum power point tracking method for photovoltaic systems. Sol Energy 2011;85(11):2965–76.
[105] Raj J, Jeyakumar A. A novel maximum power point tracking technique for photovoltaic module based on power plane analysis of i-v characteristics. IEEE Trans Ind Electron 2014;61(9):4734–45.
[106] Sher H, Murtaza A, Addoweesh K, Chiaberge M. A two stage hybrid maximum power point tracking technique for photovoltaic applications. In: Proceedings of PES general meeting — conference exposition. IEEE; 2014. p. 1–5.
[107] Murtaza AF, Sher HA, Chiaberge M, Boero D, Giuseppe MD, Addoweesh KE. A novel hybrid mppt technique for solar pv applications using perturb & observe and fractional open circuit voltage techniques. In: Proceedings of 15th international symposium on MECHATRONIKA. IEEE; 2012. p. 1–8.
[108] Sher H, Murtaza A, Noman A, Addoweesh K, Haddad KA, Chiaberge M. A new sensorless hybrid mppt algorithm based on fractional short-circuit current measurement and p&o mppt. IEEE Trans Sustain Energy 2015;6(4):1426–34.
[109] Murtaza A, Chiaberge M, Spertino F, Shami UT, Boero D, Giuseppe MD. Mppt technique based on improved evaluation of photovoltaic parameters for uniformly irradiated photovoltaic array. Electr Power Syst Res 2017;145(0):248–63.
[110] Sher HA, Rizvi AA, Addoweesh KE, Haddad KA. A single-stage stand-alone photovoltaic energy system with high tracking efficiency. IEEE Trans Sustain Energy 2017;8(2):755–62.
[111] Sher HA, Murtaza AF, Haddad KA. A hybrid maximum power point tracking method for photovoltaic applications with reduced offline measurements. In: Proceedinngs of IEEE international conference on industrial technology (ICIT); 2017. p. 1482–5.
[112] Xia LC, Qun LL. Research into maximum power point tracking method of photovoltaic generate system. In: Proceedings of international workshop on IEEE intelligent systems and applications. ISA; 2009. p. 1–4.
[113] Ponkarthik N, Murugavel KK. Performance enhancement of solar photovoltaic system using novel maximum power point tracking. Int J Electr Power Energy Syst 2014;60(0):1–5.
[114] Pandey A, Dasgupta N, Mukerjee AK. High-performance algorithms for drift avoidance and fast tracking in solar mppt system. IEEE Trans Energy Convers 2008;23(2):681–9.
[115] Sivaramakrishnan S. A novel hybrid mppt algorithm using linear extrapolation. In: Proceedings of international conference on computing and network communications; 2015. p. 643–8.
[116] Majidi SDA, Abbod MF, Raweshidy HAS. A novel maximum power point tracking technique based on fuzzy logic for photovoltaic systems. Int J Hydrog Energy 2018;43(31). [14 158–71].
[117] Femia N, Granozio D, Petrone G, Spagnuolo G, Vitelli M. Optimized one-cycle control in photovoltaic grid connected applications. IEEE Trans Aerosp Electron Syst 2006;42(3).
[118] Çelik Ö, Tekeb A. A Hybrid MPPT method for grid connected photovoltaic systems under rapidly changing atmospheric conditions. Electr Power Syst Res 2017;152(0):194–210.
[119] Batarseh MG, Za'ter ME. Hybrid maximum power point tracking techniques: a comparative survey, suggested classification and uninvestigated combinations. Sol Energy 2018;169(0):535–55.
[120] Sher HA, Addoweesh KE, Haddad KA. An efficient and cost-effective hybrid mppt method for a photovoltaic flyback microinverter. IEEE Trans Sustain Energy 2018;9(3):1137–44.
[121] Spertino F, Ahmad J, Ciocia A, Leo PD, Murtaza AF, Chiaberge M. Capacitor charging method for I-V curve tracer and MPPT in photovoltaic systems. Sol Energy 2015;119(0):461–73.
[122] Mahmoud MM. Transient analysis of a PV power generator charging a capacitor for measurement of the I-V characteristics. Renew Energy 2006;31(13):2198–206.
[123] Valencia PO, Paja CR. Sliding-mode controller for maximum power point tracking in grid-connected photovoltaic systems. Energies 2015;8(11):12363–87.
[124] Kotti R, Shireen W. Efficient MPPT control for PV sytems adaptive to fast changing irradiation and partial shading conditions. Sol Energy 2015;114:397–407.
[125] Kotti R, Shireen W. Fast converging MPPT control of photovoltaic systems under partial shading conditions. n: IEEE international conference on power electronics, drives and energy systems (PEDES); 2013.
[126] Sankar S, Mohanty M, Chandrasekaran K, Simon SP, Sood YR. high-speed maximum power point tracking module for PV systems. IEEE Trans Ind Electron 2018. [1-1].
[127] Ahmad R, Murtaza AF, Shami UT, Spertino F. An MPPT technique for unshaded/shaded photovoltaic array based on transient evolution of series capacitor. Sol Energy 2017;157(0):377–89.
[128] Kouchaki A, Eini HI, Asaei B. A new maximum power point tracking strategy for PV arrays under uniform and non-uniform insolation conditions. Sol Energy 2013;91(0):221–32.
[129] Murtaza A, Chiaberge M, Spertino F, Boero D, Giuseppe MD. A maximum power point tracking technique based on bypass diode mechanism for PV arrays under partial shading. Energy Build 2014;73(0):13–25.
[130] Chen K, Tian S, Cheng Y, Bai L. An improved MPPT controller for photovoltaic system under partial shading condition. IEEE Trans Sustain Energy 2014;5(3):978–85.
[131] Manickam C, Raman GR, Raman GP, Ganesan SI, Nagamani C. A hybrid algorithm for tracking of GMPP based on P&O and PSO With reduced power oscillation in string inverters. IEEE Trans Ind Electron 2016;63(10):6097–106.
[132] Manickam C, Raman GP, Raman GR, Ganesan SI, Chilakapati N. An Efficient global maximum power point tracking technique for a partially shaded photovoltaic string. IET Power Electron 2016;9(14):2637–44.
[133] Boztepe M, Guinjoan F, Quesada GV, Silvestre S, Chouder A, Karatepe E. Global MPPT scheme for photovoltaic string inverters based on restricted voltage window search algorithm. IEEE Trans Ind Electron 2014;61(7):3302–12.
[134] Furtado AMS, Bradaschia F, Cavalcanti MC, Limongi LR. A reduced voltage range global maximum power point tracking algorithm for photovoltaic systems Under partial shading conditions. IEEE Trans Ind Electron 2018;65(4):3252–62.
[135] Ramyar A, Eini HI, Farhangi S. Global maximum power point tracking method for photovoltaic arrays under partial shading conditions. IEEE Trans Ind Electron 2017;64(4):2855–64.
[136] Wang Y, Li Y, Ruan X. High accuracy and fast speed MPPT methods for PV string under partially shaded conditions. IEEE Trans Ind Electron 2016;63(1):235–45.
[137] Balasankar R, Arasu GT, Raj JSCM. A global MPPT technique invoking partitioned estimation and strategic deployment of P&O to tackle partial shading conditions. Sol Energy 2017;143(0):73–85.
[138] Ghasemi MA, Ramyar A, Eini HI. MPPT method for PV systems under partially shaded conditions by approximating I-V curve. IEEE Trans Ind Electron 2018;65(5):3966–75.
[139] Ahmed J, Salam Z. An enhanced adaptive P&O MPPT for fast and efficient tracking under varying environmental conditions. IEEE Trans Sustain Energy 2018;9(3):1487–96.
[140] Messalti S, Harrag A, Loukrizc. A new variable step size neural networks MPPT controller: review, simulation and hardware implementation. Renew Sustain Energy Rev 2017;68(0):221–33.
[141] Seyedmahmoudian M, Horan B, Soon TK, Rahman R, Oo AMT, Mekhilef S, Stojcevski A. State of the art artificial intelligence-based MPPT techniques for mitigating partial shading effects on PV systems – a review. Renew Sustain Energy Rev 2016;64(0):435–55.
[142] Lasheen M, Salam MA. Maximum power point tracking using Hill Climbing and ANFIS techniques for PV applications: a review and a novel hybrid approach. Energy Convers Manag 2018;171(0):1002–19.
[143] Koad RBA, Zobaa AF, Shahat AE. A novel MPPT algorithm based on particle Swarm optimization for photovoltaic systems. IEEE Trans Sustain Energy 2017;8(2):468–76.
[144] Ishaque K, Salam Z. An improved particle Swarm optimization (PSO)–based MPPT for PV With reduced steady-state oscillation. IEEE Trans Power Electron 2012;27(8):3627–38.
[145] Ishaque K, Salam Z. A deterministic particle Swarm optimization maximum power point tracker for photovoltaic system Under partial shading condition. IEEE Trans Ind Electron 2013;60(8):3195–206.
[146] Liu YH, Huang SC, Huang JW, Liang WC. A particle swarm optimization-based maximum power point tracking algorithm for PV systems operating under partially shaded conditions. IEEE Trans Energy Convers 2012;27(4):1027–35.
[147] Rajendran S, Srinivasan H. Simplified accelerated particle swarm optimization algorithm for efficient maximum power point tracking in partially shaded photovoltaic systems. IET Renew Power Gener 2016;10(9):1340–7.
[148] Li H, Yang D, Su W, Lü J, Yu X. An overall distribution particle Swarm optimization MPPT algorithm for photovoltaic system under partial shading. IEEE Trans Ind Electron 2018. [1–1].
[149] Sundareswaran K, kumar VV, Sankar P, Simon SP, Nayak PSR, Palani S. Development of an improved P&O algorithm assisted through a colony of foraging ants for MPPT in PV system. IEEE Trans Ind Inform 2016;12(1):187–200.
[150] Mohanty S, Subudhi B, Ray PK. A new MPPT design using grey Wolf optimization technique for photovoltaic system Under partial shading conditions. IEEE Trans Sustain Energy 2016;7(1):181–8.
[151] Kumar N, Hussain I, Singh B, Panigrahi BK. MPPT in dynamic condition of partially shaded PV system by using WODE technique. IEEE Trans Sustain Energy 2017;8(3):1204–14.
[152] Teshome DF, Lee CH, Lin YW, Lian KL. A modified firefly algorithm for photovoltaic maximum power point tracking control under partial shading. IEEE J Emerg Sel Top Power Electron 2017;5(2):661–71.
[153] Wu Z, Yu D. Application of improved bat algorithm for solar PV maximum power point tracking under partially shaded condition. Appl Soft Comput 2018;62(0):101–9.
[154] Sundareswaran K, Sankar P, Nayak PSR, Simon SP, Palani S. Enhanced energy output from a PV system under partial shaded conditions through artificial bee colony. IEEE Trans Sustain Energy 2015;6(1):198–209.
[155] Guo L, Meng Z, Sun Y, Wang L. A modified cat swarm optimization based maximum power point tracking method for photovoltaic system under partially shaded

condition. Energy 2018;144(0):501–14.
[156] Ram JP, Rajasekar N. A novel flower pollination based Global Maximum power point method for solar maximum power point tracking. IEEE Trans Power Electron 2017;32(11):8486–99.
[157] Kumar N, Hussain I, Singh B, Panigrahi BK. Maximum power peak detection of partially shaded PV panel by using intelligent Monkey King evolution algorithm. IEEE Trans Ind Appl 2017;53(6):5734–43.
[158] Aouchiche N, Aitcheikh MS, Becherif M, Ebrahim MA. AI-based global MPPT for partial shaded grid connected PV plant via MFO approach. Sol Energy 2018;171(0):593–603.
[159] Manickam C, Raman GP, Raman GR, Ganesan SI, Chilakapati N. Fireworks enriched P&O algorithm for GMPPT and detection of partial shading in PV systems. IEEE Trans Power Electron 2017;32(6):4432–43.
[160] Tey KS, Mekhilef S, Mahmoudian MS, Horan B, Oo AT, Stojcevski A. Improved differential evolution-based MPPT algorithm using SEPIC for PV systems under partial shading conditions and load variation. IEEE Trans Ind Inform 2018. [1–1].
[161] Lyden S, Haque ME. A simulated annealing global maximum power point tracking approach for PV modules under partial shading conditions. IEEE Trans Power Electron 2016;31(6):4171–81.
[162] Ahmed J, Salam Z. A maximum power point tracking (MPPT) for PV system using Cuckoo search with partial shading capability. Appl Energy 2014;119(0):118–30.
[163] Tang CY, Lin SH, Ou SY. Design and implementation of a hybrid maximum power point tracker in solar power system under partially shaded conditions. In: IEEE Proceedings of the 3rd international future energy electronics conference. ECCE Asia; 2017. p. 900–5.
[164] Ji YH, Jung DY, Kim JG, Kim JH, Lee TW, Won CY. A real maximum power point tracking method for mismatching compensation in PV array under partially shaded conditions. IEEE Trans Power Electron 2011;26(4):1001–9.
[165] Patel H, Agarwal V. Maximum Power Point Tracking Scheme for PV Systems Operating Under Partially Shaded Conditions. IEEE Tran Ind Electron 2008;55(4):1689–98.
[166] Hu Y, Cao W, Wu J. Thermography-based virtual MPPT scheme for improving PV energy efficiency under partial shading conditions. IEEE Trans Power Electron 2014;29(11):5667–72.
[167] Sundareswaran K, Peddapati S, Palani S. MPPT of PV systems under partial shading conditions through a colony of flashing fireflies. IEEE Trans Energy Convers 2014;29(2):463–72.
[168] Ramli MAM, Ishaque K, Jawaid F, Al-Turki YA, Salam Z. A modified differential evolution based maximum power point tracker for photovoltaic system under partial shading condition. Energy Build 2015;103(0):175–84.
[169] Sundareswaran K, Vigneshkumar V, Palani S. Development of a hybrid genetic algorithm/perturb and observe algorithm for maximum power point tracking in photovoltaic systems under non-uniform insolation. IET Renew Power Gener 2015;9(0):757–65.
[170] Luat NT, Soon LK. A global maximum power point tracking scheme employing direct search algorithm for photovoltaic systems. IEEE Trans Ind Electron 2010;57(0):3456–67.
[171] Safari A, Mekhilef S. Simulation and hardware implementation of incremental conductance MPPT With direct control method using cuk converter. IEEE Trans Ind Electron 2011;58(0):1154–61.
[172] Lian KL, Jhang JH, Tian IS. A maximum power point tracking method based on perturb and observe combined with particle swarm optimization. Ieee J Photovolt 2014;4(2):626–33.
[173] Shi J, Zhang W, Zhang Y, Xue F, Yang T. MPPT for PV systems based on a dormant PSO algorithm. Electr Power Syst 2015;123(0):100–7.